

บรรณานุกรม

- [1] E. N. Lorenz, “Deterministic non-periodic flow,” *J. Atmospheric Science*, vol. 20, pp. 130-141, 1963.
- [2] O.E. RöSSLer, “An equation for continuous chaos,” *Phys. Lett. A*, vol. 57, pp. 397–398, 1976.
- [3] O.E. RöSSLer, “An equation for hyperchaos,” *Phys. Lett. A*, vol. 71, pp. 155–157, 1979.
- [4] G. Chen and X. Dong, *From Chaos to Order: Methodologies, Perspectives and applications*, World Scientific, Singapore, 1998.
- [5] L.O. Chua, M. Komuro and T. Matsumoto, “The double scroll family,” *IEEE Trans Circuits Syst.*, vol. 33, pp. 1072–1118, 1986.
- [6] T. Matsumoto, L.O. Chua and K. Kobayashi, “Hyperchaos: laboratory experiment and numerical confirmation,” *IEEE Trans Circuits Syst.*, vol. 33, pp. 1143–1147, 1986.
- [7] L.M. Pecora and T.L. Carroll, “Synchronization in chaotic systems,” *Phys. Rev. Lett.*, vol. 64, pp. 821–823, 1990.
- [8] K.M. Cuomo and A.V. Oppenheim, “Circuit implementation of synchronized chaos with applications to communication,” *Phys. Rev. Lett.*, vol. 71, pp. 65–68, 1993.
- [9] T. Yang, C.W. Wu and L.O. Chua, Cryptography based on chaotic systems, *IEEE Trans. Circuits Syst.-I: Fundam. Appl.*, vol. 44, pp. 469–472, 1977.
- [10] M. Itoh, “Spread spectrum communication via chaos,” *Int. J. Bifurcation Chaos*, vol. 9, pp. 155–213, 1996.
- [11] M.E. Yalçın, J.A.K. Suykens and J. Vandewalle, “True random bit generation from a double scroll attractor,” *IEEE Trans. Circuits. Syst.- I*, vol. 51, pp. 1395–1404, 2004.
- [12] G. Chen, and T. Ueta, “Yet another chaotic attractor,” *Int. J. Bifurcation Chaos*, vol. 9, pp. 1465-1466, 1999.
- [13] J. Lü, G. Chen, D. Cheng and S. Čelikovský, “Bridge the gap between the Lorenz system and the Chen system,” *Int. J. Bifurcation Chaos*, vol. 12, pp. 2917–2926, 2002.
- [14] A.S. Elwakil, S. Özogus and M.P. Kennedy, “Creation of a complex butterfly attractor using a novel Lorenz-type system”, *IEEE Trans. Circuits Syst.-I*, vol. 49, pp. 527–530, 2002.
- [15] J.C. Sprott, “Simple chaotic systems and circuits”, *Am. J. Phys.*, vol. 68 pp. 758–763, 2000.
- [16] J.A.K. Suykens, A. Huang and L.O. Chua, A family of n -scroll attractors from a generalized Chua’s circuit,” *AEU. Int. J. Electron. Commun.*, vol. 51, pp. 131–138, 1997.
- [17] K.S. Tang, G.Q. Zhong, G. Chen and K.F. Man, “Generation of n -scroll attractors via sine function,” *IEEE Trans. Circuits Syst.-I*, vol. 48, pp. 1369–1372, 2001.
- [18] Y. Li, W.K.S. Tang and G. Chen, “Hyperchaos evolved from the generalized Lorenz equation,” *Int. J. Circuit Theory Appl.*, vol. 33, pp. 235–251, 2005.
- [19] A. M. Chen, J. A. Lu, J. Lü and S. M. Yu, “Generating hyperchaotic Lü attractor via state feedback Control,” *Physica A*, vol. 364, pp.103-110, 2006.
- [20] S. M. Yu, J. Lü and G. Chen, “A family of n -scroll hyper-chaotic attractors and its realizations,”

Phys. Lett. A, 2007, vol. 364, 244-251, 2007.

- [21] K. Klomkarn and P. Sooraksa, "Implement of A true Random Number Generator Using Chen's Attractor," *Proc. Int. Conf. Robot, Vision, Information, and Signal Processing*, pp.781-784, 2005.
- [22] A. Jansri, K. Klomkarn an P.Sooraksa, "Further investigation on trajectory of chaotic guiding signals for robotic systems," *Proc. Int. Symp. IEEE Communications and Information Technology*, pp.1166 – 1170, 2004.
- [23] A.Jansri, K. Klomkarn and P. Sooraksa, "On comparison of attractors for chaotic mobile robots," *Proc. IEEE Industrial Electronics Society*, pp. 2536 – 2541, 2004.
- [24] K. Klomkarn and P. Sooraksa, "Implementation on "NO CPU" Chaotic robot," *Proc. the 5th Asian Symposium on Applied Electromagnetics and Machanics*, 2005.
- [25] C. Chanvech, K. Klomkarn and P.Sooraksa, "Combined Chaotic Attractor Mobile Robots," *Int. Joint Conf. SICE-ICASE*, pp. 3079 – 3082, 2006.
- [26] S. Sakorntanant, K. Klomkarn, T. Thossansin, and P. Sooraksa, "Chaotic Mixing Biodiesel," *Inter. Conf. on Applied Science*, Vientiane, Loas, 2006.
- [27] US pat.597412 (Oct , 1999)
- [28] US pat.6266418 (Jul , 2001)
- [29] US pat.6856687 (Feb , 2005)
- [30] US pat.6907123 (Jun , 2005)
- [31] US pat.7003329 (Feb, 2006)
- [32] US pat.7210044 (Apr , 2007)
- [33] Sooraksa, P. and Klomkarn, K., An Authentication Device, World Intellectual Property Organization, WO 2008/044998 A1.

เอกสารแนบหมายเลข 1 (ภาคผนวก 1)

การประกอบและทดสอบต้นแบบขั้นสุดท้าย

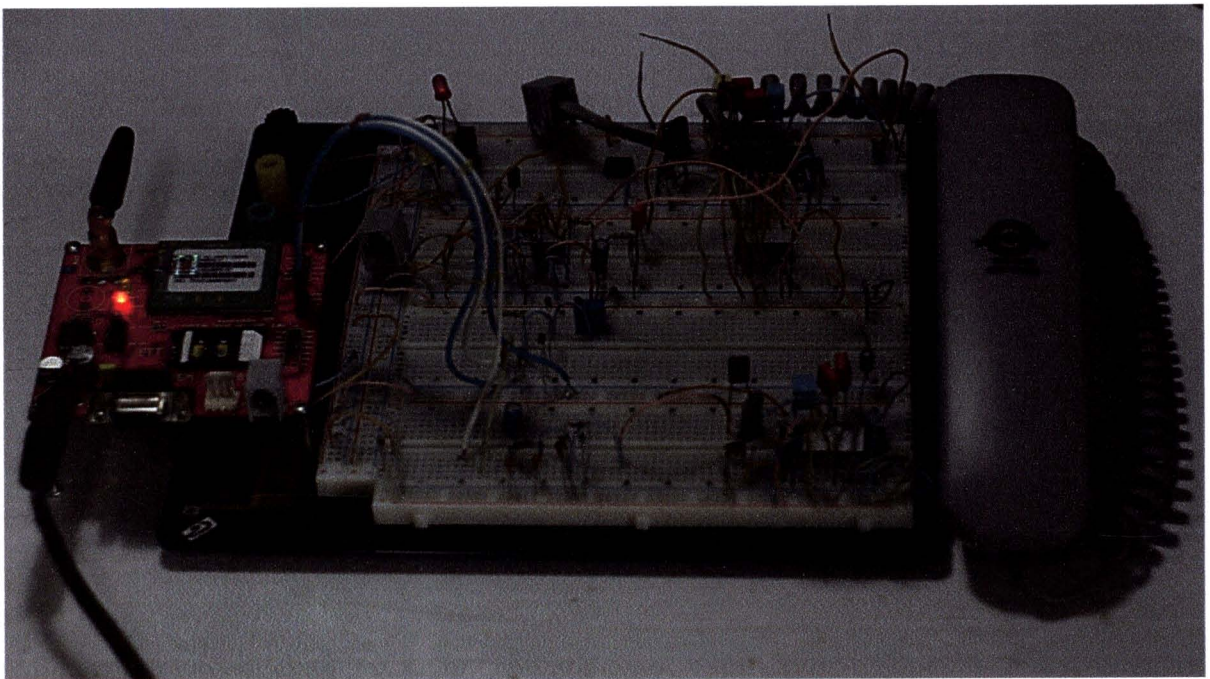
ภาคผนวก 1: การประกอบและทดสอบต้นแบบขั้นสุดท้าย

ก. เป้าหมาย

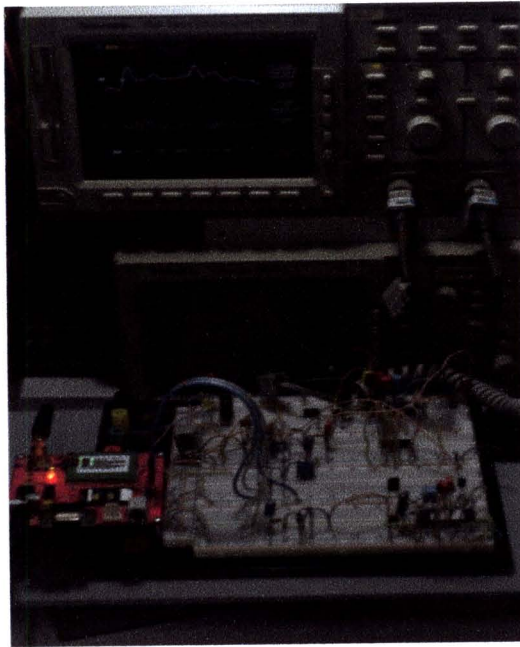
เพื่อให้ได้ผลิตภัณฑ์ต้นแบบสำเร็จพร้อมใช้

ข. ผลการทดลอง

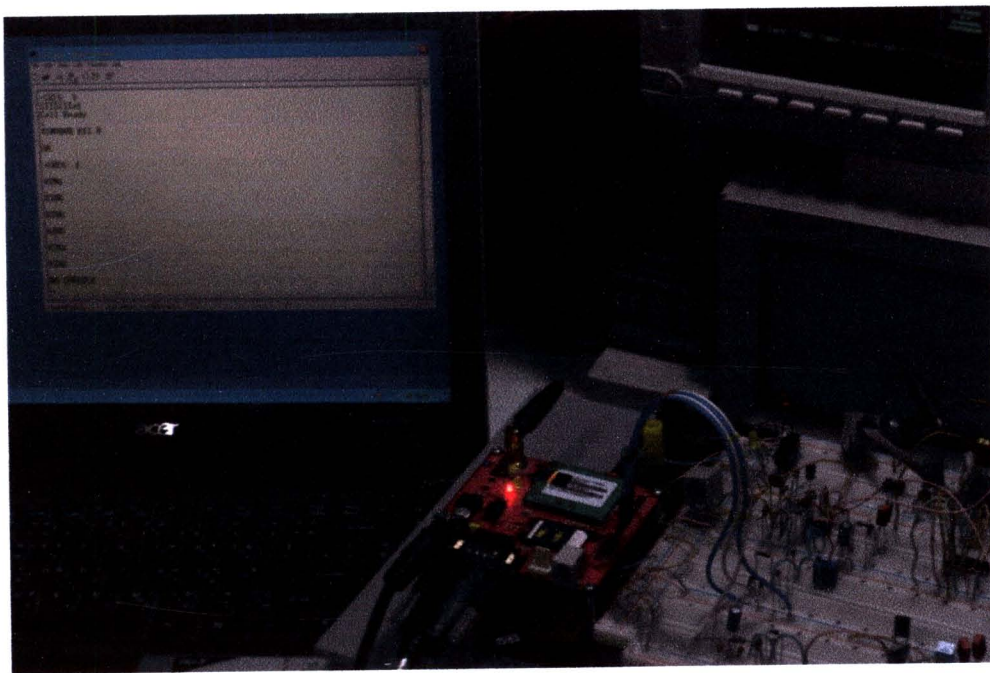
ได้นำแบบวงจรในไทรมาสที่แล้ว มาทำการสังเคราะห์สัญญาณอลวนและเชื่อมต่อกับโทรศัพท์ซึ่งประกอบชิ้นส่วนและวงจรขึ้นเองได้ผลการทดลองดังรูปที่ 1-9



รูปที่ ๑.1 วงจรจากบอร์ดทดลองในห้องปฏิบัติการก่อนทำการกัดลงแผ่น PCB



รูปที่ ๓.๒ การทดลองวัดสัญญาณจากวงจรเข้ารหัสลับเสียงโดยผ่านระบบ GSM



รูปที่ ๓.๓ การทดลองเชื่อมต่อกับคอมพิวเตอร์โดยจำลองเป็นเครือข่าย GSM

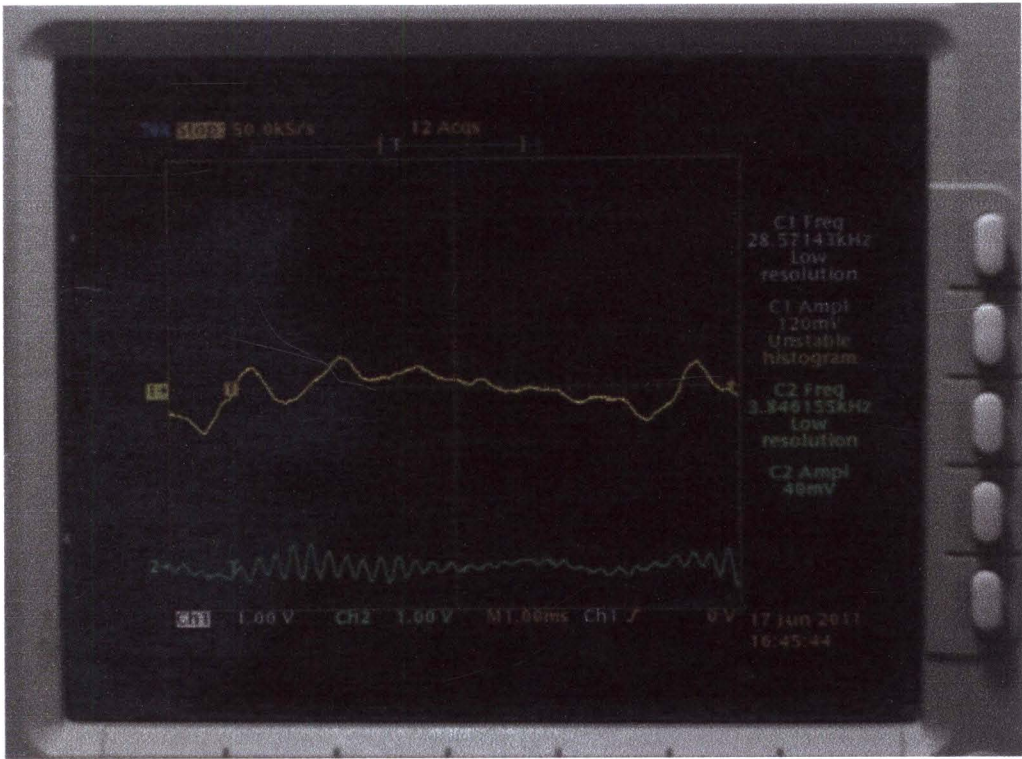
```
Test_gsm HyperTerminal
File Edit View Call Transfer Help
+CPIN: READY
+CREG: 0
+CREG: 2
Call Ready
+CREG: 1
RING
RING
RING
RING
RING
RING
ata
OK
Connected 0:01:37 Auto detect 115200 8-N-1 SCROLL CAPS NUM Capture Print echo
```



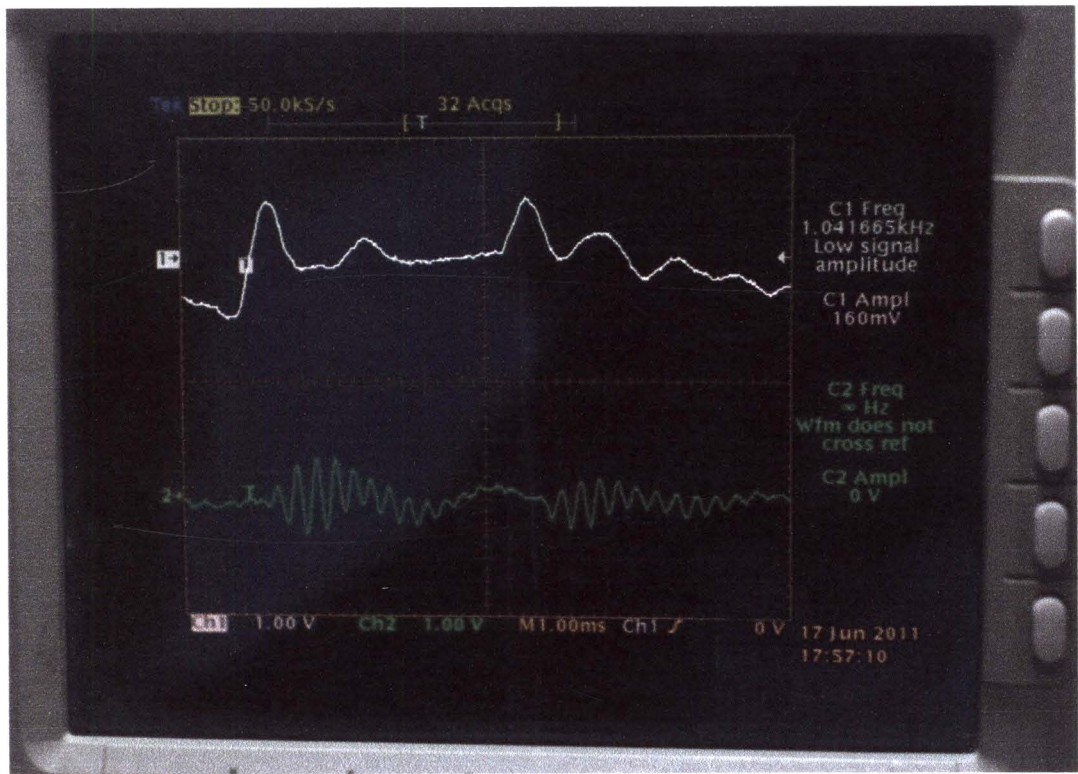
รูปที่ ๓.๔ การเรียกสัญญาณเข้าและการรับสายผ่านการทดสอบ

```
Test_gsm HyperTerminal
File Edit View Call Transfer Help
IIIIIIII
RDY
+CFUN: 1
+CPIN: READY
+CREG: 0
+CREG: 2
Call Ready
+CREG: 1
ATD0884555555;
OK
ATH
OK
Connected 0:06:43 Auto detect 115200 8-N-1 SCROLL CAPS NUM Capture Print echo
```

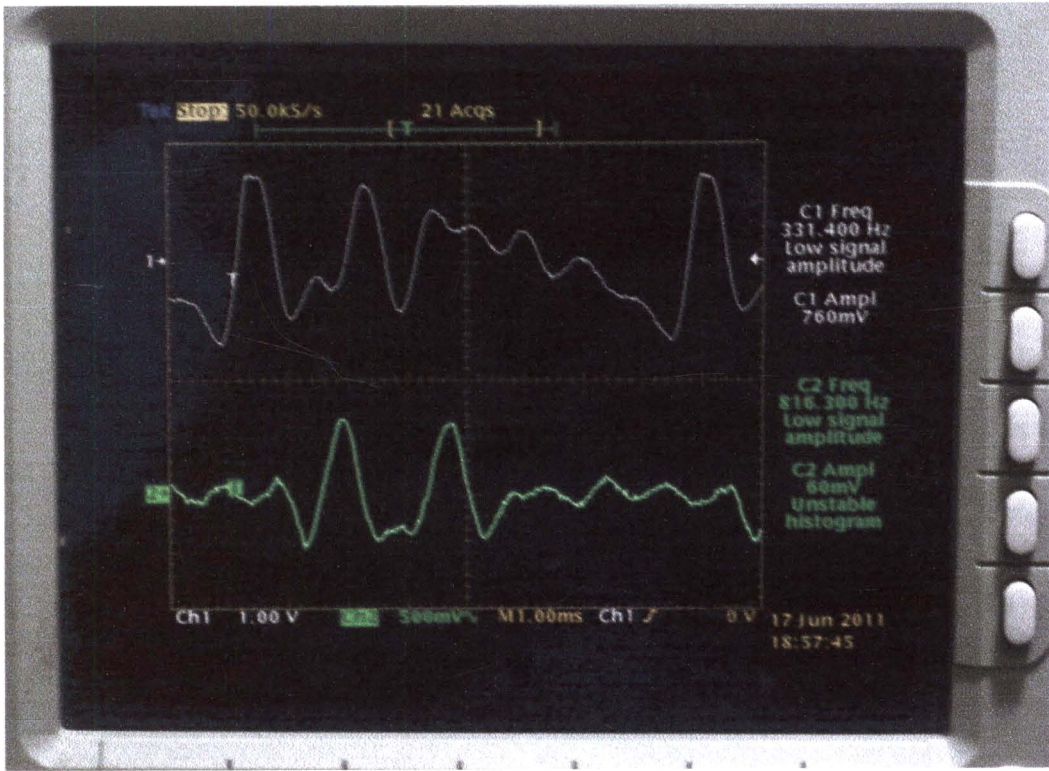
รูปที่ ๓.๕ การโทรออกและการวางสายผ่านการทดสอบ



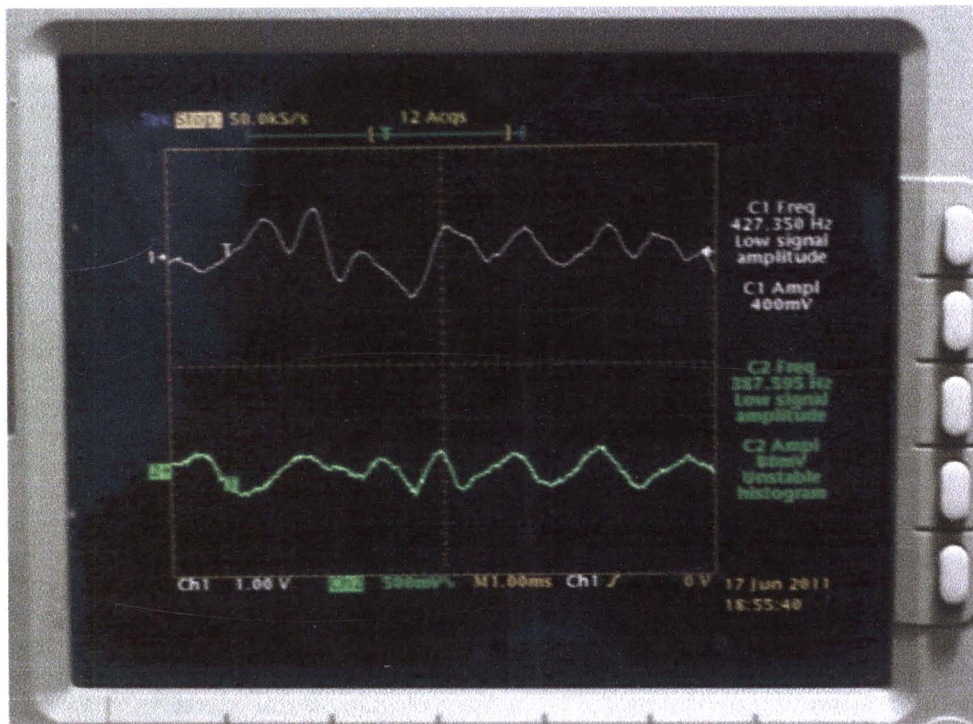
รูปที่ ๖.6 สัญญาณเสียงเข้า และเสียงที่ถูกเข้ารหัส



รูปที่ ๖.๗ สัญญาณเสียงเข้า และเสียงออกที่ไม่ถูกถอดเข้ารหัส



รูปที่ ๘.๘ สัญญาณเสียงเข้า และเสียงออกที่บายพาสผ่านวงจร



รูปที่ ๘.๙ สัญญาณเสียงเข้า และเสียงออกที่ถอดรหัสผ่านวงจร จะเห็นว่าสัญญาณพอใช้ได้ แต่จะดีขึ้นเมื่อต่อวงจรกรองสัญญาณรบกวน

ค. การทำต้นแบบ



รูปที่ ก.10 วงจรเข้ารหัสลับสัญญาณเสียงและวงจรถอดรหัสหลังลงแผ่น PCB



รูปที่ ก.11 ต้นแบบชุดที่ 1 ชุดถ่ายชุดโทรศัพท์ตั้งโต๊ะ แต่เป็น GSM เคลื่อนที่



รูปที่ ๑.๑๒ ต้นแบบชุดที่ ๒

เอกสารแนบหมายเลข 2

**ผลงานที่ได้รับการตอบรับให้ตีพิมพ์เผยแพร่ในวารสาร
International Journal of Bifurcation and Chaos (IJBC)**



SIMPLE SELF-INSTRUCTIONAL MODULES BASED ON CHAOTIC OSCILLATORS: FEW BLOCKS GENERATING MANY PATTERNS

KITDAKORN KLOMKARN* and PITIKHATE SOORAKSA†

*School of Computer Engineering, Faculty of Engineering,
King Monkut's Institute of Technology Ladkrabang,
Chalongkrung Rd., Ladkrabang, Bangkok 10520, Thailand*

**kkkitdak@kmitl.ac.th*

†kspitikh@kmitl.ac.th

Received May 20, 2010; Revised February 23, 2011

Chaotic circuits have been widely used in the teaching of nonlinear dynamics disciplines, where a common practice is pedagogically based on the circuit point of view. Chua's circuit is the most popular platform for the demonstration of its components with rich dynamical patterns. However, engineering students majoring in control systems are more familiar with feedback systems rather than physical electronics with nonlinear components. This may lead to some difficulty in understanding the nonlinear properties of Chua's circuit, at least on first sight. This paper provides an alternative approach to teaching and learning chaotic oscillators by using the inherent understanding of feedback systems with simple modules at the undergraduate level. Utilizing the idea of chaotification, which means to make a nonchaotic module chaotic, the modules consist of only four blocks yet can generate more than thirty types of chaotic patterns via their various combinations. Conceptually, the blocks can be assembled as various mixed-mode chaotic circuits. Functionally, the blocks are easy-to-use in a Simulink-like fashion. Structurally, they are a LEGO-like educational kit. With low-cost implementation employing a few op-amps for each block, the newly proposed modules are simple, self-instructional and suitable for teaching and training students in school laboratories and in experimental environments.

Keywords: LEGO; Simulink; education; chaotic oscillator; mixed-mode circuit.

1. Introduction

Exploiting chaos properties for applications in sciences is an interesting research topic in engineering community especially in various fields of electrical engineering. In electronic systems, the complex noise-like property is used to improve electromagnetic interference (EMI) in power convector [Hong *et al.*, 2010] and can be applied as testing signals both for analog and mixed-mode circuits [Ma *et al.*, 2008; Addabbo *et al.*, 2010]. In control engineering, the generated chaotic signal is utilized in path planning for mobile robots [Sooraksa & Klomkarn, 2010], enhancing the motion capability

of walking micro-robots [Buscarino *et al.*, 2007], and increasing efficiency of industrial liquid mixing processes [Zhang & Chen, 2007].

In computer and information engineering, the rich variety of dynamical behaviors can be served as a random source of cryptography [Yalcin *et al.*, 2004], and be exploited for a pattern generator in chaos computing [Ditto *et al.*, 2008]. In communication engineering, synchronized property is a great source producing potential applications for radar [Liu *et al.*, 2007] and secure communication [Tam *et al.*, 2006].

As far as the above applications are concerned, the study of chaotic dynamics for the undergraduate

majoring in electrical engineering has become important and is a powerful tool to transform fundamental knowledge into chaotic products for creative economy. A question is how to give lecture and set up a laboratory experiment such that a concept of design and construction chaos is clear, concise, and coherent with engineering nature. Starting from the engineering point of view, the design and construction of chaotic circuit as major building tool boxes for the applications are practical in order to introduce the student to understand chaotic dynamics and related behaviors. In [Tam *et al.*, 2006], a chaotic oscillator for education purpose is presented by introducing the third-order autonomous chaotic oscillator modified from a formal sinusoidal oscillator. Although the circuit contains a few elements, easy-to-build and simple-for-measurement, it only exhibits a single scroll attractor. To obtain a variety of chaotic dynamical behaviors, the well-known Chua's circuit is an excellent example, it is a useful education tool for high school students to learn and play creating fascinating music and amazing arts from the chaotic attractor [Bilotta *et al.*, 2010]. For a computer based laboratory setup at undergraduate student level, PC Chua [Tôrres *et al.*, 2005] that demonstrates control and synchronization by a personal computer, is proposed. For an intensive study and implementation, the practical guide to construct Chua's circuit in Field Programmable Analog Array: FPAA, presenting mix-mode chaos and guiding to laboratory setup, can be found in the monograph [Kiliç, 2010].

However, Chua's circuit concept lies on a circuit based design. The circuit consists of a nonlinear negative resistor and passive components such as resistors, capacitors and requires one inductor. For a student, when conducting a hands-on laboratory experiment, starting with the circuit is easy when constructing but may be difficult in re-scaling frequency. In addition, for those who are beginners, the circuit does not easily realize a suitable inductor without prior knowledge of an equivalent gyrator. Trying to understand behaviors of a nonlinear element in the circuit without a background in physical electronics or electromagnetics may be a bit of a challenge.

In fact, the students are already familiar with the second-order linear system in fundamental engineering courses such as differential equation, signal and systems, automatic control or feedback control. Embracing the concept of the second-order one, and extending by adding one more integrator

to the system, a chaotic system can be achieved by applying the Poincare Bendixson theorem [Hirsh & Smale, 1974]. The theorem states a necessary condition for an n -dimensional continuous vector field to be chaotic; to obtain such a system, n must be greater or equal to 3. Adopting this concept, the construction of a chaotic circuit in the laboratory becomes simple when a lecturer starts teaching with a background concept of the second-order system, and then extending to the third-order nonlinear system with Poincare Bendixson theorem. In other words, a chaotic system can be obtained by chaotification transforming the second-order ordinary system to be the third-order chaotic system with a feedback loop [Tang & Zhong, 2003]. To visualize the chaotic dynamical behaviors throughout the chaotification process, before carrying out an experiment, students are encouraged to use graphical software such as MATLAB/Simulink [Chaturvedi, 2010] to simulate chaotic systems.

This paper presents an alternative approach to enhance the effectiveness of laboratory pedagogy by using chaotification approach instead of introducing Chua's circuits to undergraduate students for the construction and understanding of chaotic phenomena. To achieve this objective, the functional level electronic design as module based chaotic circuit introduced in [Yu *et al.*, 2007] is adopted. In [Yu *et al.*, 2007], the module provides three-scroll and butterfly attractor scrolls. Unlike [Yu *et al.*, 2007], instead of using multiplier device in nonlinear modules, we adapt the module by using simple nonlinear devices designed as Simulink-like function blocks with only four simple blocks and three external sources. Structurally the four blocks have a LEGO-like structure consisting of a core module possessing the property of the second-order linear system, an auxiliary module having an extended integrator and two nonlinear modules. Possible combination of selecting elements out of the four provides four main chaotic models and various chaotic mixed-mode attractors ranging from a single scroll to complex scroll chaotic attractors. Apparently more than 30 chaotic patterns are obtained.

This paper is organized as follows. In Sec. 2, three autonomous chaotic systems and two nonautonomous chaotic systems used in the experiment are reviewed. Providing both pulse and sine drives for the nonautonomous system in this paper can be considered as some extension of the past research illustration of module-based chaotic circuits design. In other words, the multiscroll patterns generated

by a sine wave drive is fulfils the gap of missing members in the collection of complete modules. This point alone is one of the contributions by the authors besides creating the new educational kit. Four main models derived from typical forms of chaotic equations are also briefly illustrated. Some example of Simulink model and the simulation results are provided as well. In Sec. 3, the electronic circuits implemented in each module are explained. A combination of utilizing the modules from the models for generating a chaotic attractor is demonstrated in Sec. 4, while the results are shown in Sec. 5. Section 6 concludes the paper.

2. System Models

In this section, a brief review of four typical chaotic forms called system equations or system models is presented as a basic guideline for the study. A family of chaotic signals can be easily generated by varying the parameters of the model and combining them. From system perspective, each model can be viewed as a block library containing designed parameters. The main models are presented as follows.

2.1. Model I: The third-order autonomous chaotic system I

In order to construct a third-order circuit with nonlinear feedback concept for laboratory experiment, a family of simple chaotic circuits can be written in a single third-order ordinary differential equation called “jerk equation,” introduced by Sprott [2000]. The families of the simple Sprott’s circuit using a few operational amplifiers (OAs) and simple nonlinear elements, provided single or double-scroll attractors, are easy to construct. To realize a simple Sprott’s circuit, [Elwakil & Kennedy, 2001] shows that integrator summer architecture with the signum function as a nonlinear feedback can be realized to generate double scroll-like chaotic attractors. To increase the number of scroll attractors from the jerk architecture, generating a grid scroll chaotic attractor using hard limit series as nonlinearity was suggested by [Yalcin *et al.*, 2002]. For another implementation to increase the complexity of the attractor, YU and others [Yu *et al.*, 2005] proposed a nonlinear modulating function to generate n -scroll attractors. However, generating double scroll and complex scroll from the general jerk

or the modified general jerk circuit as appeared in [Elwakil & Kennedy, 2001; Yalcin *et al.*, 2002] using the relatively expensive current conveyor were exploited. And in [Yu *et al.*, 2005], the coefficients of the linear circuit require on adjustment of precision, not being easy to realize in the laboratory experiment at an undergraduate level.

In this paper, we simplify the construction of the third-order autonomous chaotic system which can obtain a wide range of chaotic signals from a single scroll to complex scrolls by only jumping the connectors and adding an external driving function in the laboratory test bed. The proposed model, Model I, is specified as follows:

$$\begin{bmatrix} x' \\ y' \\ z' \end{bmatrix} = \begin{bmatrix} 0 & 1 & 0 \\ -1 & a & 1 \\ 0 & 0 & -1 \end{bmatrix} \begin{bmatrix} x \\ y \\ z \end{bmatrix} + \begin{bmatrix} y_p(t) \\ 0 \\ f(x) + x_p(t) \end{bmatrix} \quad (1)$$

where $f(x) = a$ nonlinear function, a is the rate of divergence of an unstable system, and $x_p(t)$, $y_p(t)$ are optional external driving pulse functions.

The system equation (1) consists of the third-order linear system, a nonlinear element and driving pulses. In linear system, states x and y are the second-order unstable subsystems. Adding the state as a hyperplane, the third-order nonlinear dynamical system in (1) is dissipative, and has a negative eigenvalue and a pair of complex conjugates with positive real part. The equilibrium point $(0, 0, 0)$ is an index-2 spiral-saddle point. Since the system is unstable on the x - y plane, the trajectory scrolls are away from the equilibrium point. To fold the trajectories, nonlinear elements in Eqs. (2a)–(2d) can be employed. In Model I, the Heaviside function in Eq. (2a) is applied to obtain a single scroll, while the signum function in Eq. (2b) and the hysteresis function in Eq. (2c) are enforced to generate double scrolls. To assign single or double scroll, the saturating function in Eq. (2d) can be used for generating chaotic signals by threshold control [Lü *et al.*, 2008]. The method is as simple as adjusting the gain of the amplifier in the system. To generate multi-scroll attractors, the staircase function in Eqs. (2e₁) and (2e₂) together with external driving pulse functions $x_p(t)$ and $y_p(t)$ are used to alter the equilibrium of the system. All nonlinear functions used herein are summarized as:

$$H(x) = \begin{cases} 1 & x \geq 0 \\ 0 & x < 0 \end{cases} \quad (2a)$$

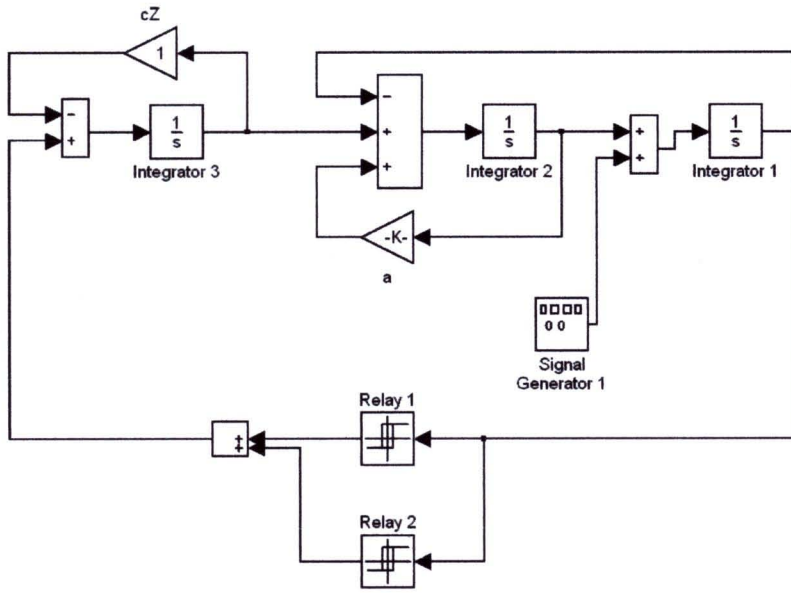


Fig. 1. Simulink model of the third-order autonomous chaotic system I, Model I, with the staircase function using Eq. (2e₁).

$$\text{sgn}(x) = \begin{cases} 1 & x \geq 0 \\ -1 & x < 0 \end{cases} \quad (2b)$$

$$\text{hys}(x) = \begin{cases} +1 & -1 < x < \infty \\ -1 & -\infty < x < 1 \end{cases} \quad (2c)$$

$$\text{sat}(x) = \begin{cases} 1 & x > L \\ kx & |x| < L \\ -1 & x < -L \end{cases} \quad (2d)$$

where $L = |x/k|$, k is amplifier gain,

$$f(x) = 2\{\text{sgn}(x + v_1) + \text{sgn}(x - v_1)\} \quad (2e_1)$$

$$f(x) = \{\text{sgn}(x) + \text{sgn}(x + v_1)\text{sgn}(x - v_1)\} \quad (2e_2)$$

and v_1 is the reference voltage associated with the creation of the new equilibrium. In order to explain the relative structure between Simulink models and the module based chaotic oscillators, Fig. 1 gives an example of Simulink model for the simulation of Model 1. Based on our experiences, the students can use the nonlinear function in Eq. (2e₁) with the external driving signal to generate a 6-scroll chaotic attractor. We encourage the reader to simulate and figure out the parameters to obtain such a system as a good exercise. Note that, in the simulation model, integrator, amplifier and summing building blocks are provided and some of the nonlinear functions such as the signum and the saturation building blocks can be selected from the math operation and discontinuity block library of Simulink.

The Heaviside and the hysteresis functions can be setup from the relay block diagram.

In Fig. 1, the nonlinear equation (2e₁) is represented by summing output Relays 1 and 2 in which parameter setup is shown in Table 1, the amplitude and frequency of $y_p(t)$ is ± 1 and 0.2 rad/s, the simulation result of the Simulink model is depicted in Fig. 2(c). To illustrate more effects on selecting the nonlinear functions, Figs. 2(a) and 2(b) show simulation results of system equation (1) with the Heaviside and the signum function, respectively. As can be seen from the figures, choices of nonlinearity alter the equilibrium and folding patterns of the trajectories. All simulations set parameter a representing the rate of divergence of an unstable system equal to 0.085.

2.2. Model II: The third-order autonomous chaotic system II

In the previous subsection, we investigate that using the signum function in Model I, the state space of

Table 1. Setup parameter for relays of the Simulink model in Fig. 1.

Relay	SW On Point	SW Off Point	O/P When On	O/P When Off
1	2	2	4	0
1	2	2	4	0

Note that O/P stands for outputs.

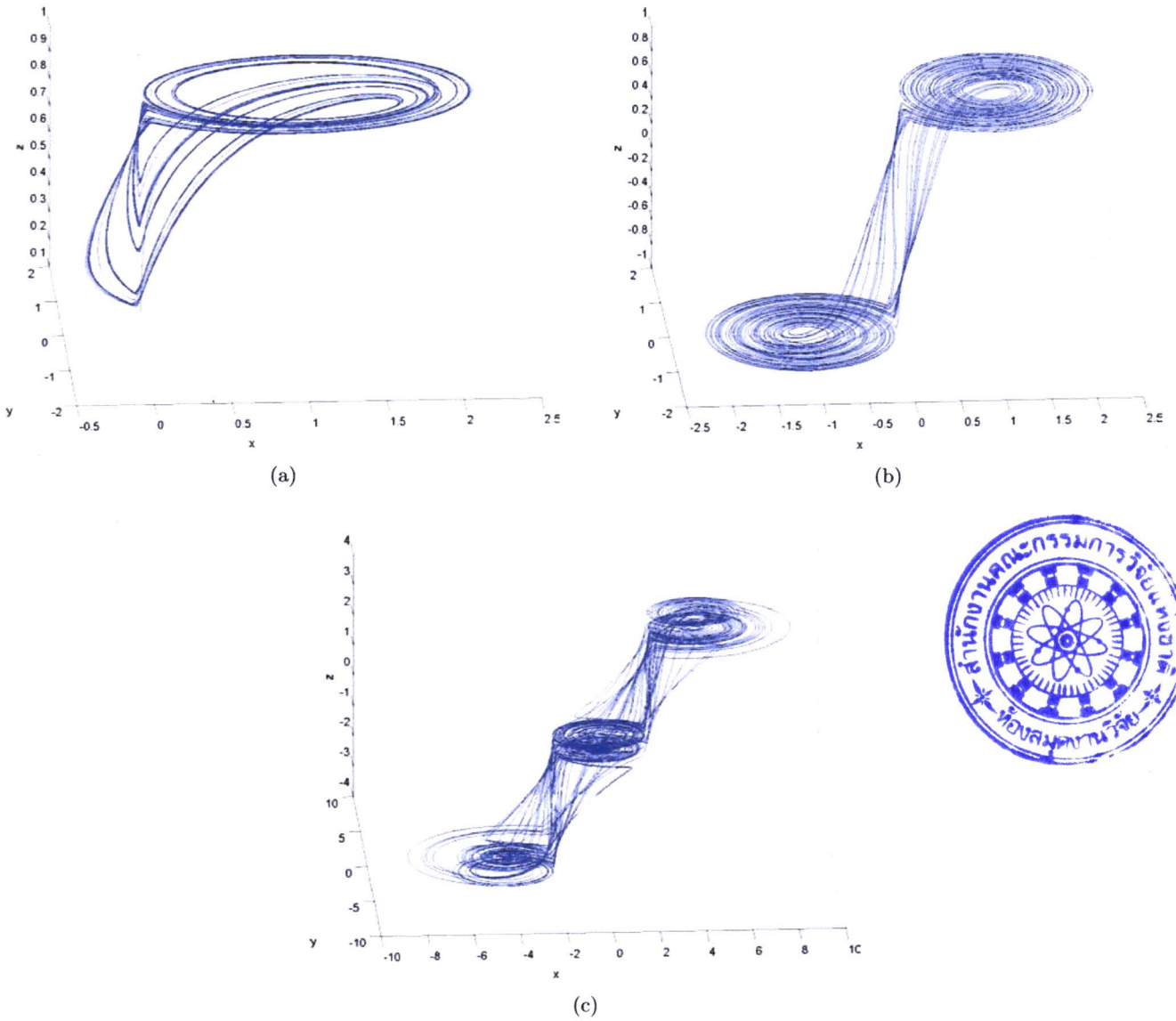


Fig. 2. Simulink simulation results of Model I: (a) with the Heaviside function, (b) with the signum function, (c) with the staircase function ($2e_1$).

the system is divided into two subsystems by separating in parallel to the z -axis. Applying the outcome by extending the one-dimensional z -axis onto the two-dimensional x - z plane and using a similar approach, the third-order chaotic system of the modified type can be expressed as

$$\begin{bmatrix} x' \\ y' \\ z' \end{bmatrix} = \begin{bmatrix} 0 & 1 & 0 \\ -1 & a & 0 \\ 0 & 0 & -1 \end{bmatrix} \begin{bmatrix} x \\ y \\ z \end{bmatrix} + \begin{bmatrix} y_p(t) \\ f(x+z) \\ f(x+z) \end{bmatrix} \quad (3)$$

where $f(x+z)$ is a nonlinear function, $y_p(t)$ is an optional external driving pulsed signal. To generate double scrolls, we set $f(x+z)$ as the signum

function of Eq. (2b). In similar manner, the multi-scroll chaotic attractors can be obtained by using

$$f(x+z) = 2\{\text{sgn}(x+z+v_1) + \text{sgn}(x+z-v_1)\} \quad (4a)$$

$$f(x+z) = \frac{1}{2}\{\text{sgn}(x+z) + \text{sgn}(x+z+v_1) \times \text{sgn}(x+z-v_1)\}. \quad (4b)$$

The staircase functions in Eqs. (4a) and (4b) are modified from the staircase functions in Eqs. (2e₁) and (2e₂) with scaling factor 1/2.

Note that the eigenvalues of Model II possess the same property as those of Model I, except the

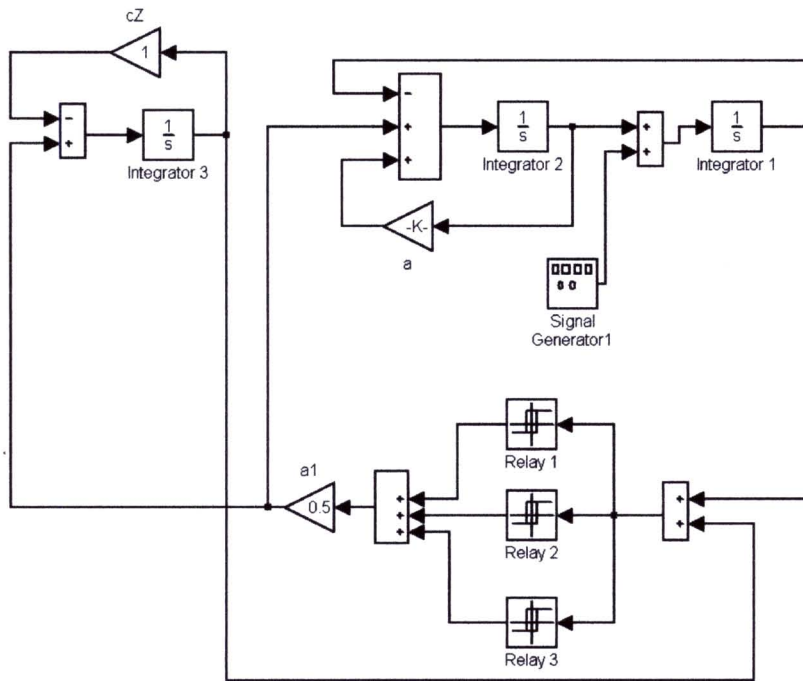


Fig. 3. Simulink model of the third-order autonomous chaotic system II, Model II, with the staircase function (4a).

system has coupled the state z by feeding it back to the nonlinear function. In simulation, Simulink model of Model II employing the nonlinear function (4b) with the external driving signal $y_p(t) = \pm 0.5$ is illustrated in Fig. 3. The summing of signal outputs of Relays 1–3 with scaling 1/2 are obtained corresponding to the nonlinear function in Eq. (4b). Setup parameters for the relays are shown in Table 2.

An 8-scroll chaotic attractor obtained from the system in Fig. 3 is shown in Fig. 4(b). A simplified version of the nonlinear function as the signum function $f(x + z)$ can be shown by the double-scroll pattern in Fig. 4(a).

2.3. Model III: The second-order autonomous chaotic system

To demonstrate a simple chaotic oscillator, the second-order autonomous chaotic system is

exploited and the state equation can be described as:

$$\begin{bmatrix} x' \\ y' \end{bmatrix} = \begin{bmatrix} 0 & 1 \\ -1 & a \end{bmatrix} \begin{bmatrix} x \\ y \end{bmatrix} + \begin{bmatrix} 0 \\ hys(x) \end{bmatrix} \quad (5)$$

where $hys(x)$ is the hysteresis function and a is the rate of divergence of an unstable system which equals to 0.085.

This system is proposed in [Cook, 1985] and has a simple structure. A detailed study of chaotic behaviors corresponding to Model III is presented in [Moreno *et al.*, 2001]. The model consists of an unstable second-order linear system with a hysteresis feedback. This linear system has complex conjugate eigenvalues on the right-half plane (RHP) with two unstable focuses on the x - y plane providing a stretch mechanism for the dynamic trajectory. The hysteresis element can be used as a switch or folding mechanism to excite the trajectory to another unstable plane. Since the model is obviously a simple system, computer simulation is not provided in this subsection. The readers are referred to [Cook, 1985; Moreno *et al.*, 2001] for more information. However, experimental results corresponding to Model III are given in Sec. 4. It is worth noting that, during a laboratory class, the lecturer may mention about the hardware realization corresponding to this model which may be simple as a flip-flop with two comparators forming a memory.

Table 2. Setup parameter for relays of the Simulink model in Fig. 3.

Relay	SW On Point	SW Off Point	O/P When On	O/P When Off
1	0	0	1	-1
2	2	2	2	0
3	-2	-2	0	-2

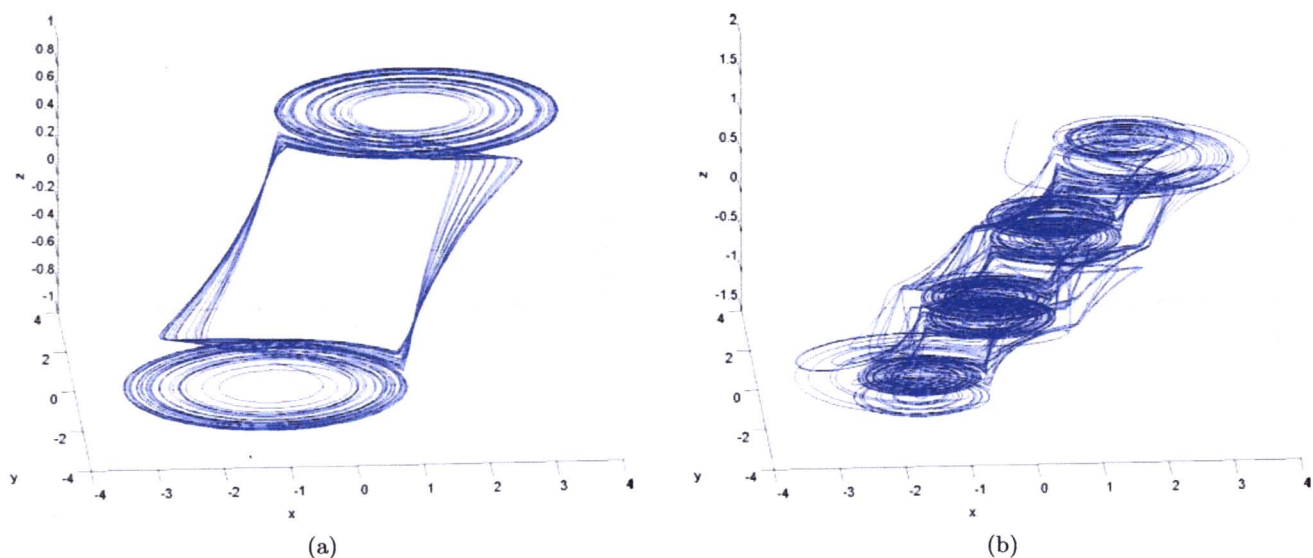


Fig. 4. Simulation results of Model II: (a) with the signum function, (b) with the staircase function (4b).

2.4. Model IV: The nonautonomous chaotic oscillator

In the previous subsections, all models are autonomous types. This subsection presents Model IV which is a nonautonomous chaotic oscillator. To generate a chaotic attractor from a nonautonomous system, the system consists of the second-order linear circuit and a nonlinear element in the feedback loop is driven by time-varying sinusoidal signal [Mykolaitis *et al.*, 2000]. The system is realized by a comparator as the signum function [Mykolaitis *et al.*, 2000] implying the potential application in secure communication [Milioua *et al.*, 2007]. A different approach in realizing the system can be achieved by exploiting a saturating amplifier as a threshold controller for the nonlinear element [Mohamed *et al.*, 2010].

To model the module based chaotic oscillator, the nonautonomous chaotic oscillator system is constructed by using the equation:

$$\begin{bmatrix} x' \\ y' \end{bmatrix} = \begin{bmatrix} 0 & 1 \\ -1 & -a \end{bmatrix} \begin{bmatrix} x \\ y \end{bmatrix} + \begin{bmatrix} f(x) \\ f_s(\omega t) \end{bmatrix} \quad (6)$$

where $f_s(t)$ can be selected as sinusoidal or periodic pulse driving signals with angular velocity ω .

The system equation (6) consists of the second-order stable linear system with a sign function in the feedback loop driven by the sinusoidal signal. The system can generate a double-scroll chaotic attractor. We can also modify the system to obtained multiscrolls by using the nonlinear function as described in Eqs. (2e₁) and (2e₂).

In [Ozoguz & Elwakil, 2004], the sinusoidal force is replaced by pulse excitation and can be proved that strange attractors exist in the system. This can be done by adding the sign for a nonlinear transconductor. The nonautonomous chaotic system illustrated in Eq. (6) is a dissipative system and can be analyzed as the fourth-order autonomous chaotic system by transforming the sinusoidal and pulse forcing functions into a second-order system.

To demonstrate some simulation examples, Simulink model of Model IV with sinusoidal driving signal that exploit the nonlinear function in Eq. (2e₂) having parameters as in Table 1 is shown

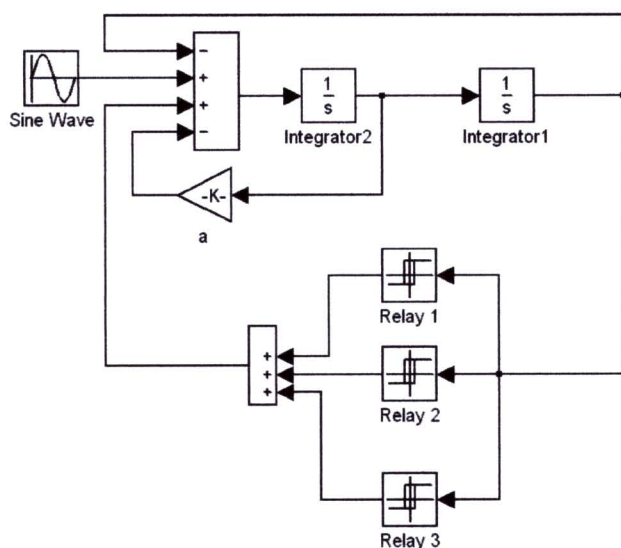


Fig. 5. Simulink model of the nonautonomous chaotic system, Model III, with the staircase function using Eq. (2e₂).

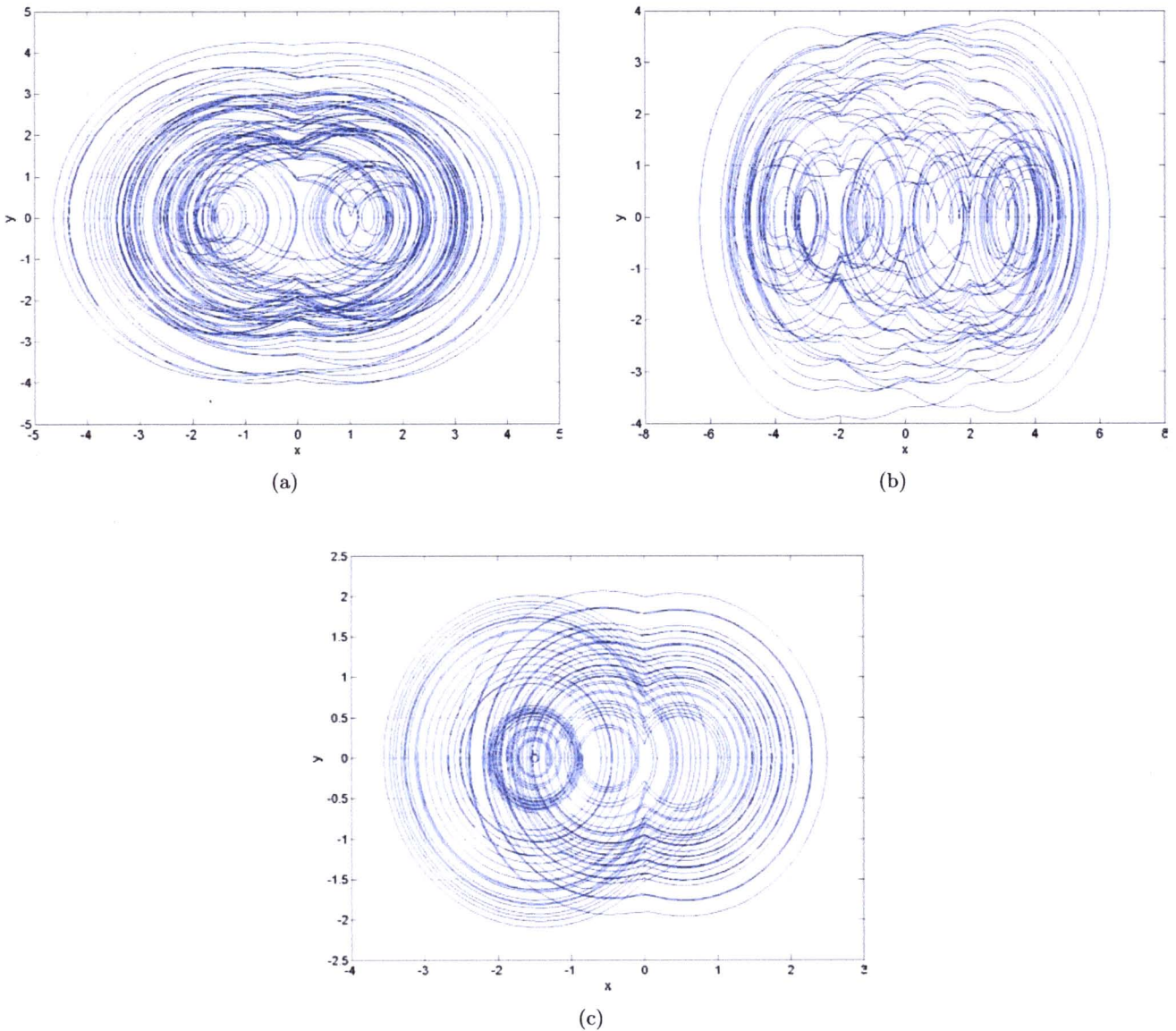


Fig. 6. Simulation results of the nonautonomous chaotic system, Model IV: (a) with the signum function driven by sinusoidal signal, (b) with the staircase function (4b) driven by sinusoidal signal, (c) with the Heaviside function driven by pulse signal.

in Fig. 5, where the simulation result is shown in Fig. 6(b). The damping coefficient of second-order system is -0.025 and the amplitude and frequency of the sinusoidal wave are 1 and 1.1 rad/s, respectively. For the case of using the signum function as the nonlinear element with sinusoidal driving signal, a double-scroll attractor in Fig. 6(a) is obtained. Figure 6(c) shows the use of the Heaviside function and pulse driving signal with setup amplitude and frequency equal to $\pm 0.5, 0.2$ rad/s, respectively. We will see later that the simulation results obtained in this section agreed with experimental results by using the modules in the next section.

3. Circuit Modules

Instead of starting from circuits to systems, our approach in this section is for a top down designed educational material — from systems to circuits. According to Gestalt psychology [Gray, 2010], we realize that the learning perception is best understood as an organized whole pattern rather than as separate parts. In this section, we describe how to design and construct circuit modules based on the guideline of the system models in the previous section.

From Simulink diagrams, the main block diagrams in Figs. 1–3 are the second-order linear

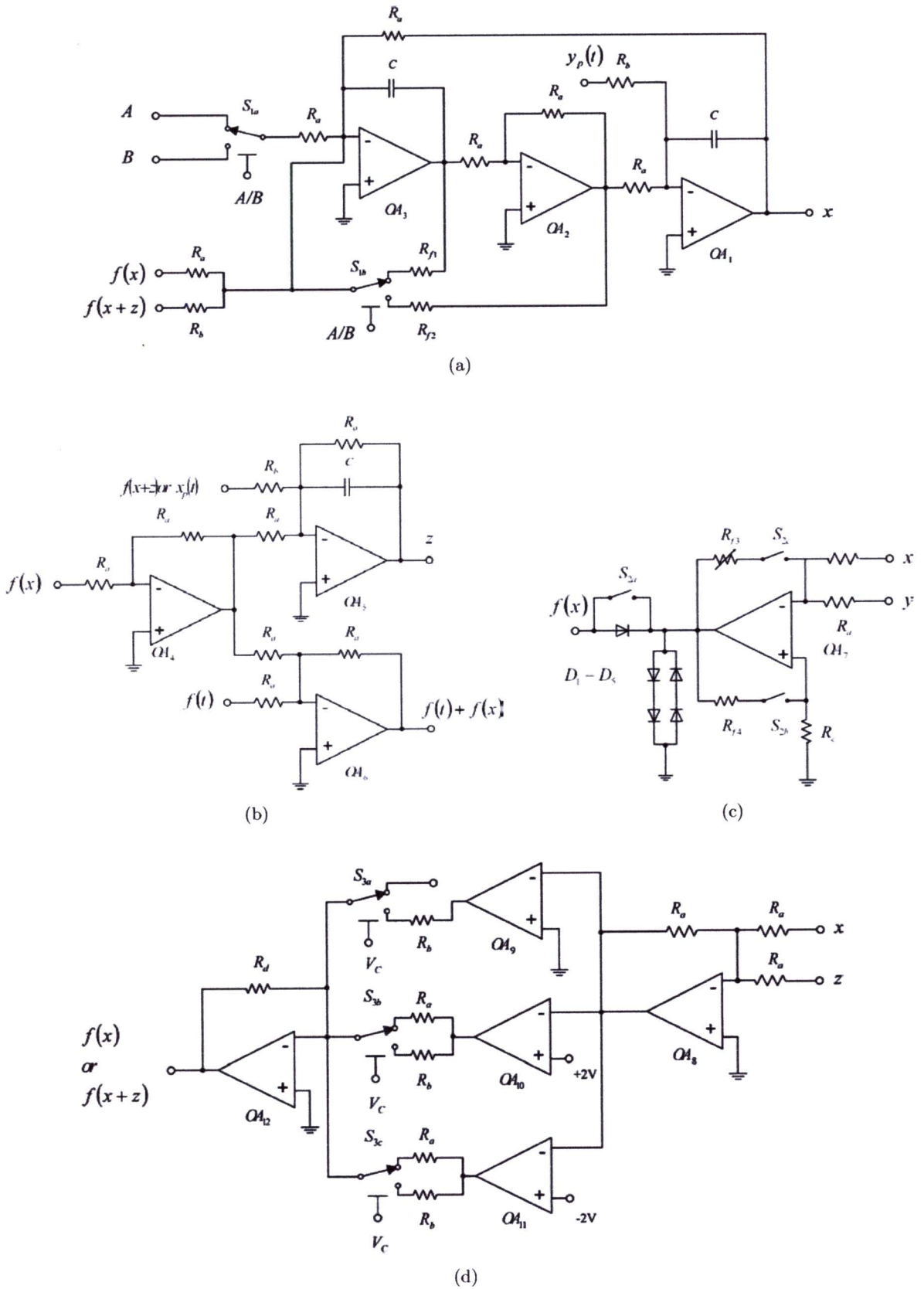


Fig. 7. Experiment modules: (a) Module A: The two-integrator loop module, (b) Module B: The extended integrator module, (c) Module C: The programmable nonlinear function module, (d) Module D: The staircase function module.

system consisting of two integrators and feedback coefficient amplifiers. For an autonomous chaotic system in Figs. 1 and 2, the third integrator is used to extract the third-order linear system. For each simulation in the previous section, the nonlinear block is assigned by using Eqs. (2a)–(2d) to obtain a single scroll or double scroll. Similarly, Eqs. (2e₁), (2e₂), (4a) and (4b) are assigned to obtain a multi-scroll chaotic attractor.

Therefore in the experimental setup, the four modules of circuits depicted in Fig. 7 are implemented to accomplish the construction of all proposed models in the previous section. These four modules are described in the following.

3.1. Module A: The two-integrator loop module

This main module, Module A, is depicted in Fig. 7(a) used for assigning the states x and y of the linear systems in Eqs. (1), (3), (5) and (6). The second-order system is the main part of the linear system for Models III and IV and is a subsystem used for connecting with the state z in the linear part of Models I and II. This circuit module consists of an inverting integrator OA₁, an inverting amplifier OA₂ and a summing inverting integrator OA₃. It is a closed-loop second-order system, where the states x and y are outputs of OA₁ and OA₃. And the output of state x is a feedback input of itself. In order to assign the complex conjugate poles moving between the LHP and the RHP, the coefficients of the output of the state y can be selected by using an analog multiplexer. The negative and positive coefficients are defined as Rf_1 and Rf_2 respectively. The time constant of an integrator setting frequency of the chaotic oscillator is $1/R_a C$. To connect the main module with another module, the input terminals A and B selected by an analog multiplexer can be used to connect with the linear function in Module B. Pins $f(x)$ and $f(x+z)$ are used for connecting with the nonlinear function in Module C.

3.2. Module B: The extended integrator module

This module is shown in Fig. 7(b). The module consists of a lossy integrator and a summing amplifier. The integrator is implemented by OA₅ and a resistor R_a and a capacitor C used for the extension of a second-order module to a third-order linear system. The summing amplifier OA₆ is designed for a

mixed-mode operation by adding a signal from the nonlinear device and the driving signal generator.

3.3. Module C: The programmable nonlinear function module

In this module, OA₃ shown in Fig. 7(c) is assigned as a nonlinear function. To activate the Heaviside, the sign, the saturate and the hysteresis functions, this can be done by setting switches 2a–2c to select the feedback resistor and the output voltage of the OA. The operational functions of switches are shown in Table 3.

Because voltage bias of OA is in the range of ± 15 V, and the saturation output is in the operational range of ± 13.5 V; therefore, suitable diodes D1–D4 are identified as 1N914 which can be used to limit the voltage of the nonlinear function and to scale the behavior of the chaotic signals.

3.4. Module D: The staircase function module

The module is depicted in Fig. 7(d). Module D consists of operational amplifiers: OA₉–OA₁₁ which are realized as nonlinear functions described by Eqs. (2e₁), (2e₂), (4a) and (4b) to set the equilibriums of chaotic systems of Models I, II and IV. Detail configuration for composing the circuit modules to be a system model via interconnection is shown in Sec. 4. To make a module functional as Eqs. (2e₁) and (4a) or as Eqs. (2e₂) and (4b), this can be done by setting analog multiplexers S_{3a} – S_{3c} to connect with resistors R_a and R_b accordingly. For all functional modules, an operational amplifier LF 351 is supplied with ± 15 V supply voltage. The analog multiplexer in use is an IC CD4052 having two inputs multiplexed with the ± 12 V supply voltage functioning as an automatic switch. The switch enables the student to select the desired input as can be seen from the output later in the next section that the three- or four-chaotic scrolls can be obtained accordingly.

Table 3. Parameter configuration of switches for activation of selected function.

Function	S_{2a}	S_{2b}	S_{2c}
Heaviside	Off	Off	Off
Signum	On	Off	Off
Saturate	On	Off	On
Hysteresis	On	Off	Off

Note that circuit components used throughout this paper are: $R_a = 10\text{ k}\Omega$, $R_b = 20\text{ k}\Omega$, $R_c = 50\text{ k}\Omega$, $R_d = 1.5\text{ k}\Omega$, $R_{f4} = 50\text{ k}\Omega$, and $C = 3\text{ nF}$.

4. Modules to Models

In previous sections, we first presented a whole picture of the chaotic systems as models in Sec. 2 and then described separated elements of the designed circuits as the block modules in Sec. 3. For logical presentation throughout this paper, we apply the reasoning structure in dynamic programming using the Bellman’s optimality principle [Lewis & Syrmos, 1995] to achieve optimal learning. The key idea suggests that after working backward from the goal to the initial point as the top-down approach, we then work forward from the initial point to complete the goal as the bottom up approach. Analogically, adopting the Gestalt’s learning concept [Gray, 2010], the top down pedagogy is proposed in the transition from Secs. 2 and 3. The transition from Secs. 3 and 4 can be considered as the bottom up learning process in dynamic programming establishing a progressive learning for students.

To benefit from psychological learning theory, this section has adopted the “learning-by-doing” concept in the progressive learning theory founded by John Dewey [1938]. Knowing properties of each block modules from Sec. 3, this section presents how the circuit Modules A–D based on chaotic oscillators can be composed to construct the system Models I–IV spanning from autonomous chaotic

system, nonautonomous chaotic system to mixed mode chaotic ones. The known property of each block is a self-instruction in the sense of LEGO-like style. The combination is dependent on the designer where the choices are free to be chosen. For example, some selected six chaotic system models can be established by using the four circuit block modules. The demonstration is performed as follows.

4.1. Experimental set up for Model I

To set up the third-order autonomous chaotic system, Model I, the two-integrator loop module or the main module or Module A and the extended integrator module or Module B are used to compose the assigned system. For a nonlinear version, the model can be achieved by combining the third-order linear system with a programmable nonlinear function or Module C. Output choices to be single or double scrolls are dependent on the assigned function which can be the Heaviside, the signum, the saturate or the hysteresis functions. The connection diagram and the block layout of this experimental set-up are shown in Fig. 8. Here, for the main module, the analog multiplexer is set to position A in order to operate in unstable mode. The connection diagram shows that output of the main module is connected to the input x of the nonlinear module. And the output z of the extended integrator module is connected to input A of the main module. Finally, the programmable nonlinear function

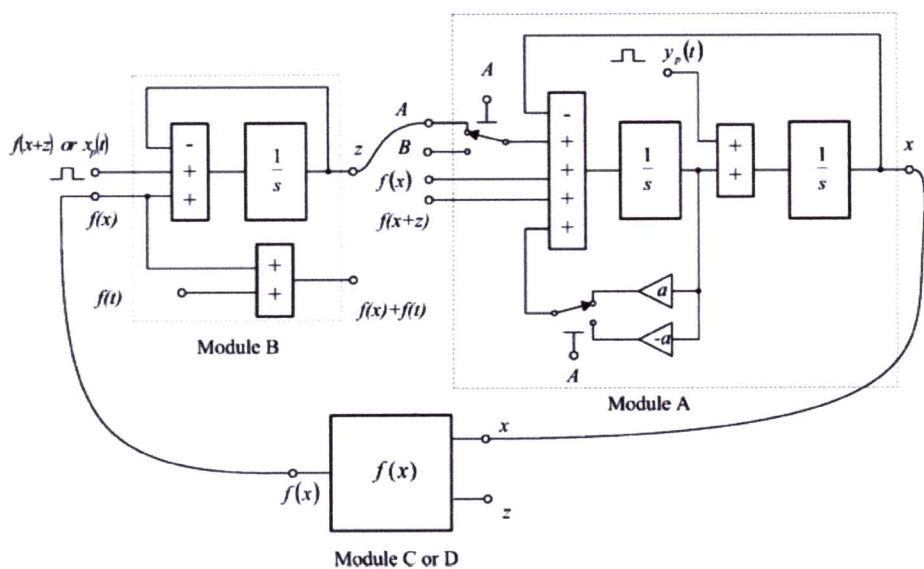


Fig. 8. Experimental set up for Model I.

module output is connected to input $f(x)$ of the extended integrator module.

To set up the multiscroll attractor, the stair case function module, Module D, is used as a nonlinear function instead of selecting the programmable nonlinear function, Module C. In this experiment, the complexity of the chaotic attractor can be increased by applying the external driving pulse signal with amplitude ± 2 to the inputs $x_p(t)$ and $y_p(t)$ of the extended integrator and the main module to extend more scrolls in the x and y axes, respectively.

4.2. Experimental set up for Model II

In the experiment of the third-order autonomous chaotic system in Model II, all modules are used to compose the required system as shown in Fig. 9. To exhibit a double-scroll attractor, an analog multiplexer in the main module (Module A) is set to position A and the programmable nonlinear function (Module C) is set to be the signum function. In order to set up a multiscroll chaotic oscillator, the stair case function module (Module D) is used as a nonlinear function to obtain 3 or 4 scrolls. The connection diagram of this experiment is shown in Fig. 9, according which, the output of the staircase function module (or the programmable nonlinear function module) is connected to the input $f(x+z)$ of the main module and the extended integrator module (Module B). In this operational configuration, the system can increase scrolls in the y axis by driving

the pulse signals with magnitude ± 1 V at the input $y_p(t)$ of the main module.

4.3. Experimental set up for Model III

In this configuration, the main module (Module A) and the programmable nonlinear function module (Module C) are used for setting up the experiment. The experimental configuration is illustrated in Fig. 10. In the figure, the analog switch in the main module is set to position A for exhibiting an unstable second-order linear system and the programmable nonlinear function module is assigned for the hysteresis function.

4.4. Experimental set up for Model IV

In this experiment, the set up for the nonautonomous chaotic oscillator can be divided into two schemes. The first scheme shown in Fig. 11, a nonautonomous chaotic oscillator using pulse excited with the Heaviside or the signum function as a nonlinear function is set up by using the main module and the programmable nonlinear function. From the system equation of Model IV, a second or a linear system is a stable system. To achieve this mode, the analog multiplexer is set to position B. The 1 kHz square wave pulsed with amplitude ± 1 V is applied to excite an input (B) of the main module.

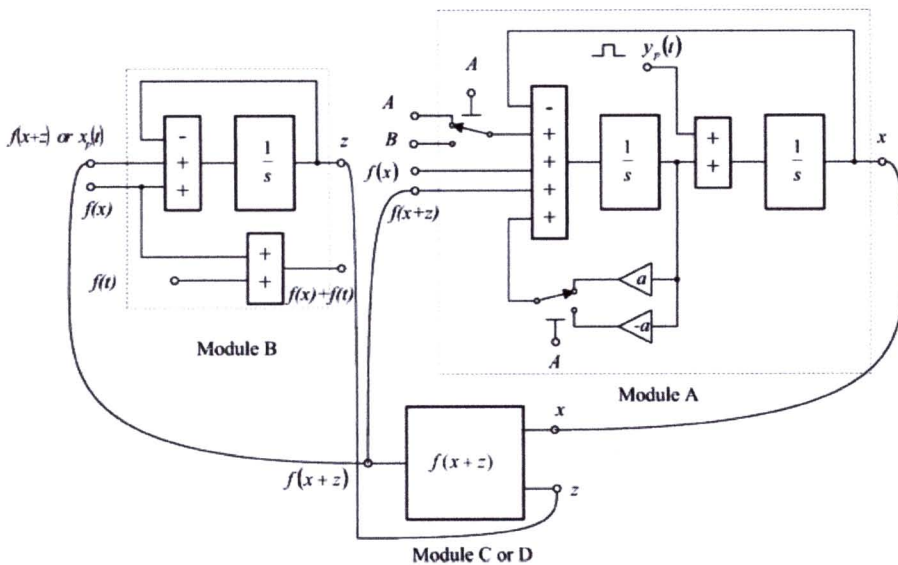


Fig. 9. Experimental set up for Model II.

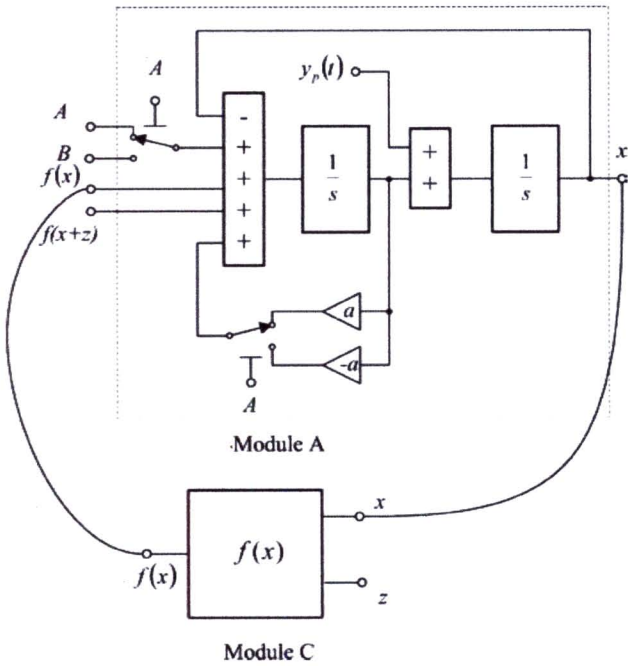


Fig. 10. Experimental set up for Model III.

In the second scheme, a nonautonomous chaotic system with a sinusoidal driver can be obtained. The double scrolls can be achieved when using the programmable nonlinear function module as the signum function. Likewise, the system exhibits three or four scrolls when using the staircase function module.

The experimental set up configuration is the same as the first scheme except the sinusoidal signal

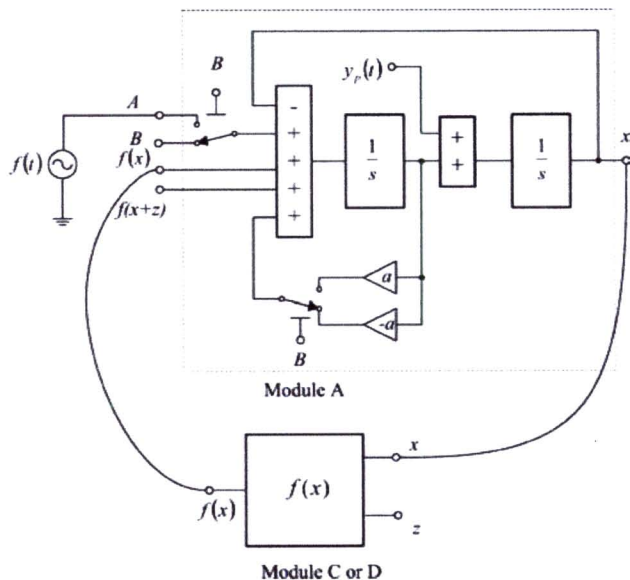


Fig. 11. Experimental set up for Model IV.

is applied to excite at input B of the main module. And the staircase function module is used as a non-linear function for the experimental set up to obtain the 3- or 4-scroll chaotic oscillator.

4.5. Experimental set up for the mixed-mode chaotic oscillators

In this experiment, the module based chaotic system can be set up to generate a mixed-mode chaotic oscillator exhibiting behaviors in between Models I and IV. In other words, the mix-mode model can be generated by hybridizing or interconnecting the main module, the extended integrator and the programmable nonlinear function modules. Alternatively, the programmable nonlinear function module can be interchanged with the stair case function module. In the main module, analog multiplexers S_{1a} and S_{1b} can be switched between inputs A or B and between unstable or stable by controlling from the external pulse signal driver at the terminal A/B. Variation of the mixed-mode schemes are demonstrated as follows.

In the first scheme, the mixed mode lies in between an autonomous chaotic system in Model I and a nonautonomous chaotic system with the driving pulse signal in Model IV. In this mode, the programmable nonlinear function module is set as the Heaviside or the signum function. The scheme is shown in Fig. 12. In the figure, the driving pulse generator and the output of the nonlinear module are connected to inputs $f(t)$ and $f(x)$, respectively. Output of the extended integrator $f(x)+f(t)$, which is added between the signal from the nonlinear module and the driving pulse, is connected to terminal B of the main module. And the output z of the extended or the third-order integrator is connected to terminal A of the main module. The switched control signal applied to the control terminal A/B has square pulses with ± 12 V amplitude.

For the second mixed-mode scheme, the autonomous chaotic system in Model I is mixed with the nonautonomous chaotic system in Model IV and with the sinusoidal driving pulse signals using the signum function as a nonlinear element. The configuration of this scheme is the same as shown in Fig. 12 but the sinusoidal signal is applied to the terminal $f(t)$ of the extended integrator instead.

The third mixed-mode scheme is multiscroll chaos that occurs in between an autonomous chaotic system in Model I and a nonautonomous

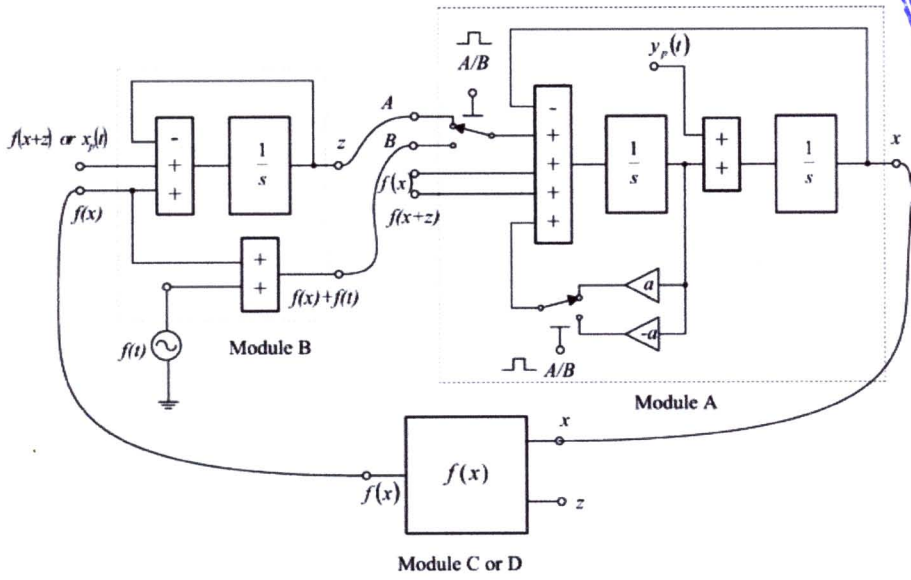


Fig. 12. Experimental set up for a mixed mode chaotic oscillator.

system in Model IV by selecting the staircase non-linear function used together with the main and the extended integrator models.

4.6. Experimental set up of the pseudo 7-scroll chaotic attractor

The last demonstration for the experimental set up in this section is the pseudo 7-scroll chaotic

oscillator. To achieve this mode, Model I or Model II consisting of the main module, the extended integrator and the staircase functions can be composed together. The pseudo 7-scroll pattern is exhibited by swapping back and forth between the 3-scroll and 4-scroll modes, as the name implies. Due to the limitation of the human eyes, the pattern seems to be appear in seven scrolls by our visual memory illusion. An analog multiplexer in the staircase module is controlled by the external pulse signal generator.

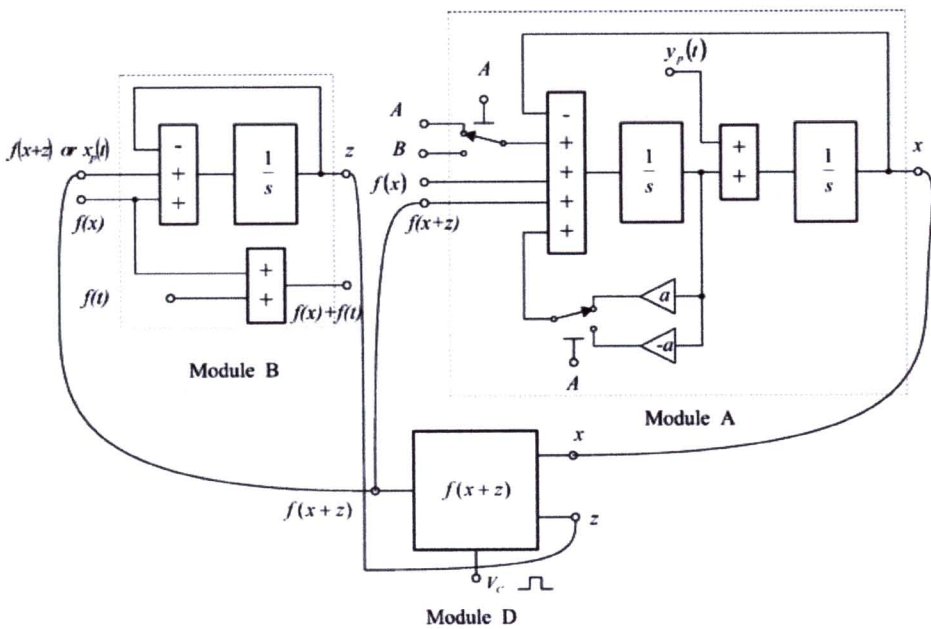


Fig. 13. Experimental set up for the pseudo 7-scroll chaotic oscillator.

The amplitude and the frequency of switching pulse in the mixed-mode and the pseudo 7-scroll experiment set up are ± 12 V and 200 Hz. The configuration of this mode is exhibited in Fig. 13. Experimental results from the module block topology in this section will be presented in the next section.

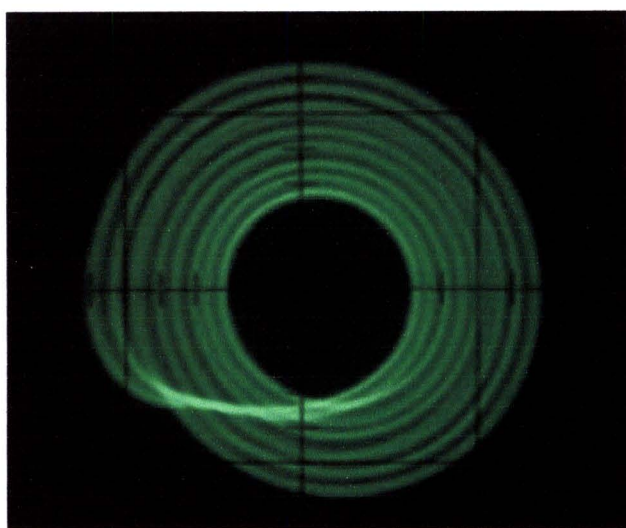
5. Experimental Results

From the experimental set up in Sec. 4, various chaotic models can be obtained by using

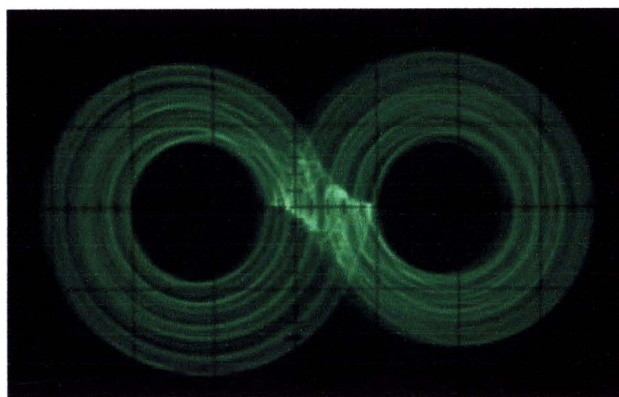
the designed block modules. This section aims to present experimental results in accordance with some selected possible configurations of using block modules presented in the last section.

5.1. Results from Model I

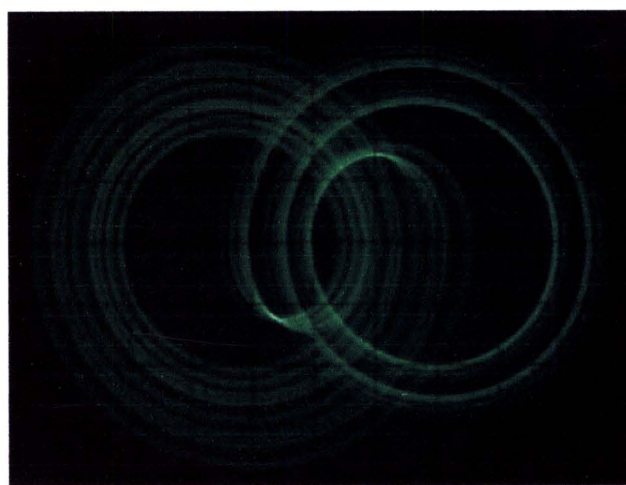
To begin with, the third-order autonomous chaotic system of Model I that provides a single-scroll or double-scroll chaotic attractor can be obtained by setting the programmable nonlinear function in a



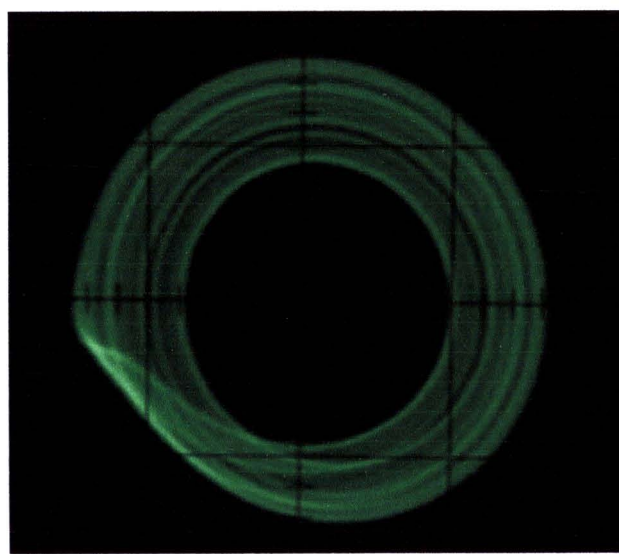
(a)



(b)



(c)



(d)

Fig. 14. Experimental results of the chaotic circuits of Model I: (a) using the Heaviside function, (b) using the signum function, (c) using the hysteresis function, (d) using the saturate function gain $k = 5.2$, (e) using the saturate function gain $k = 7$, (f) using the signum function with the ± 1 V driving pulse at $x_p(t)$, (g) using the signum function with the ± 1 V driving pulse at $y_p(t)$. Note that, for all subfigures, we set $x = 1$ V/div and $y = 1$ V/div.

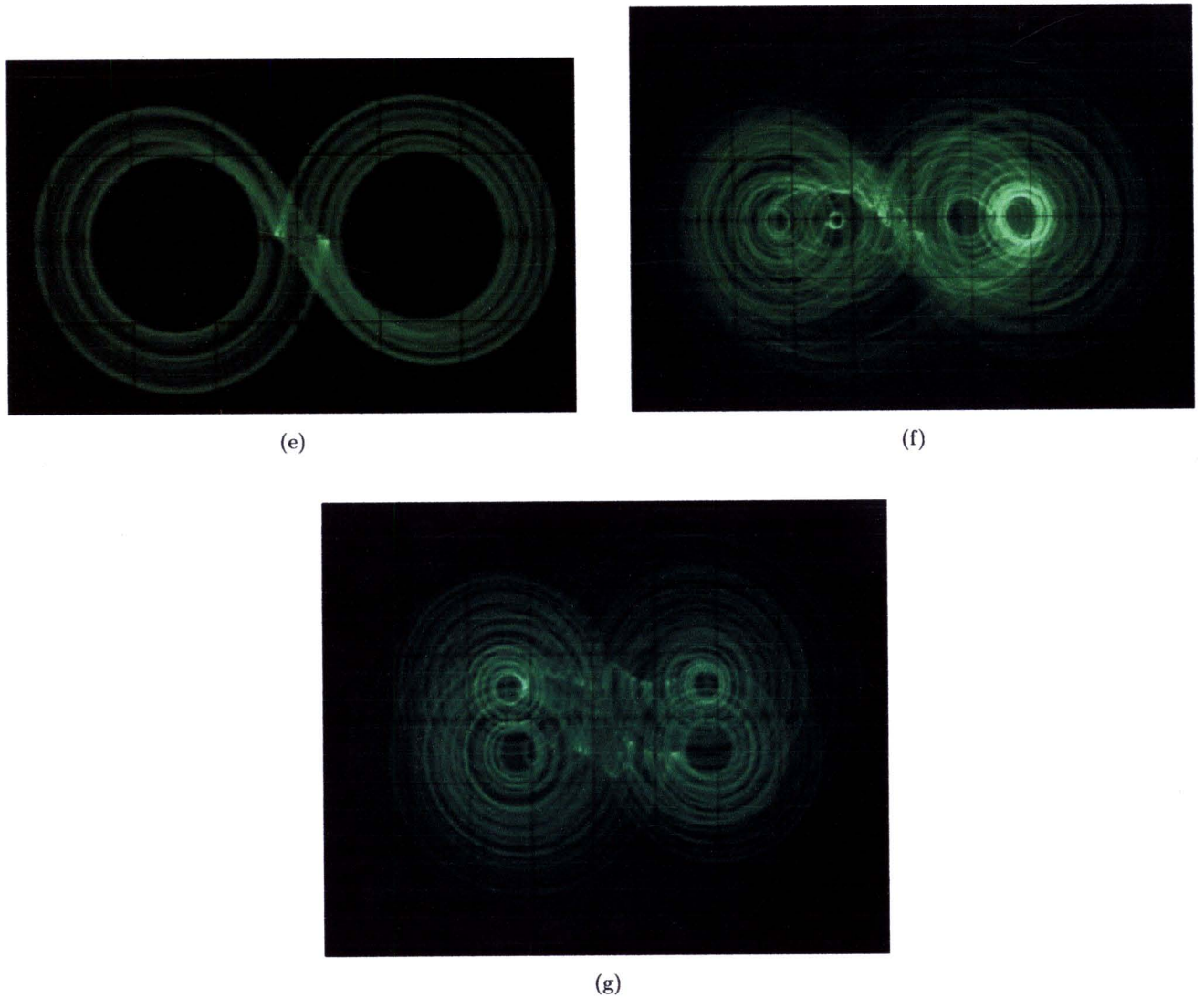


Fig. 14. (Continued)

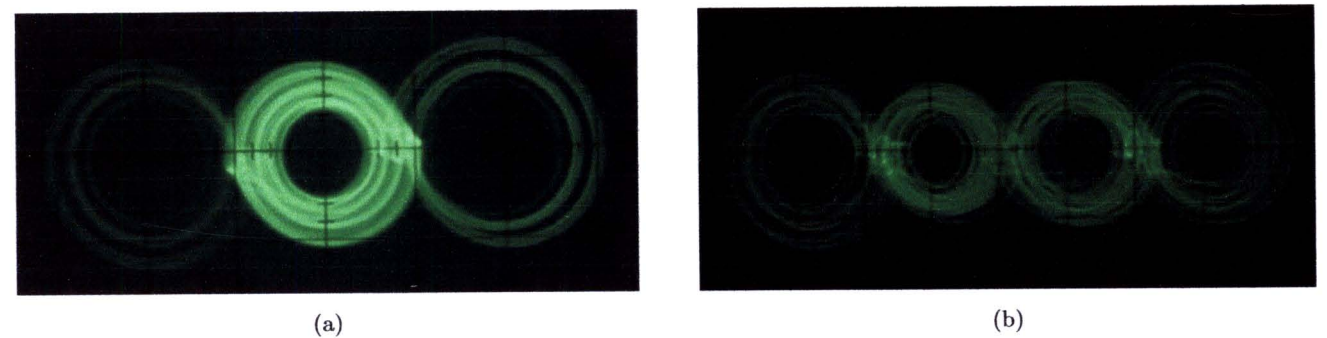
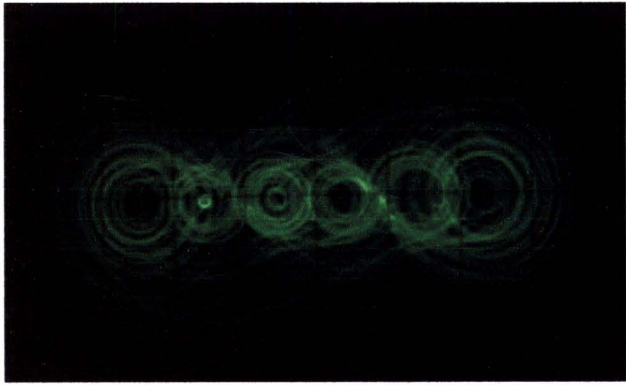
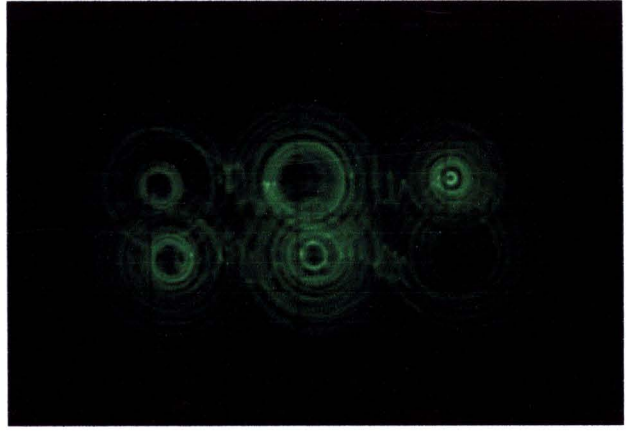


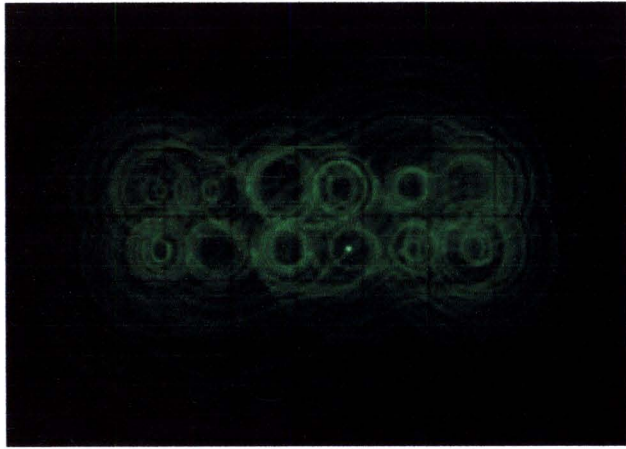
Fig. 15. Experimental results of the multiscroll chaotic circuits of Model I: (a) using the staircase function ($2e_1$), (b) using the staircase function ($2e_2$), (c) using the staircase function ($2e_1$) with the ± 2 V driving pulse for $x_p(t)$, (d) using the staircase function ($2e_1$) with the ± 2 V driving pulse for $y_p(t)$, (e) using the staircase function ($2e_1$) with the ± 2 V driving pulse for both $x_p(t)$ and $y_p(t)$, (f) using the staircase function ($2e_1$) with the ± 2 V driving pulse for $x_p(t)$, (g) using the staircase function ($2e_2$) with the ± 2 V driving pulse for $y_p(t)$, (h) using the staircase function ($2e_2$) with the ± 2 V driving pulse both for $x_p(t)$, $y_p(t)$. Note that the axes of subfigures (a)–(e): $x = 2$ V/div and $y = 2$ V/div and for (f)–(h): $x = 1$ V/div and $y = 2$ V/div.



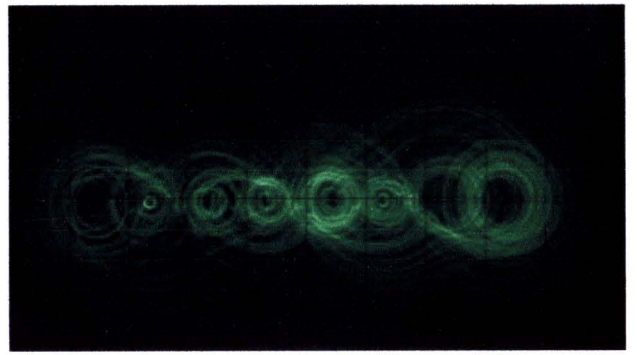
(c)



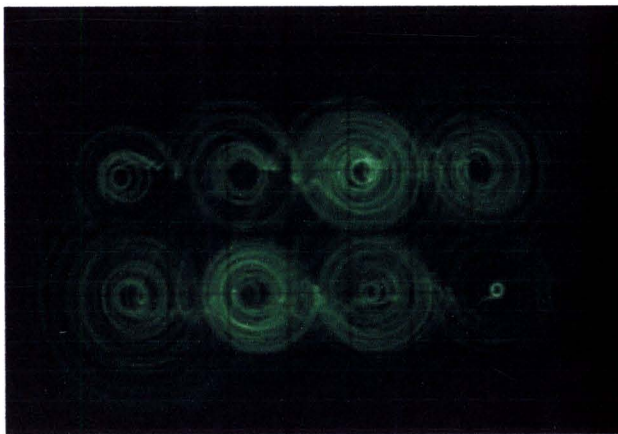
(d)



(e)



(f)



(g)

Fig. 15. (Continued)

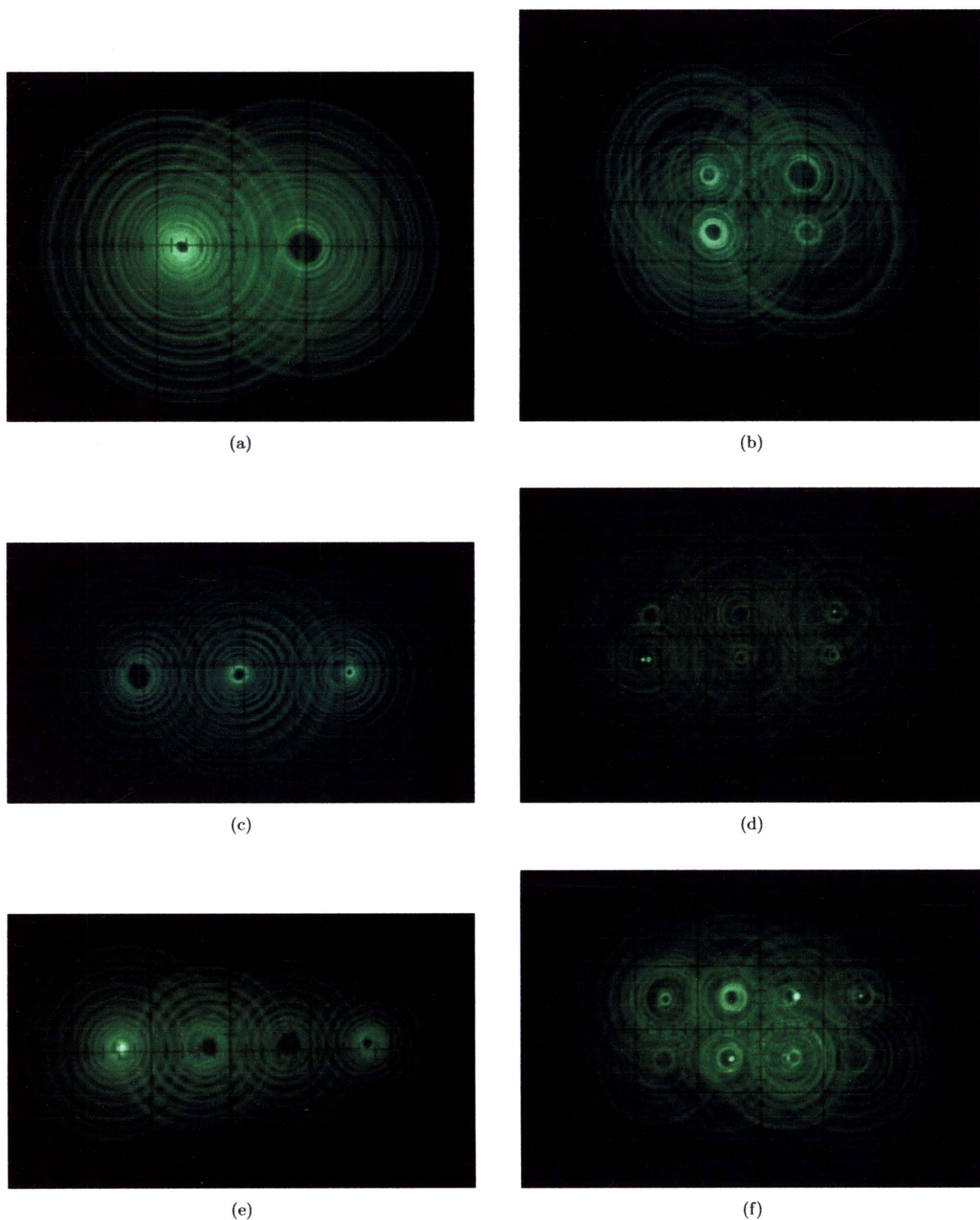


Fig. 16. Experimental results of the setup system Model II: (a) using the signum function, (b) using the signum function with the 1V driving pulse for, (c) using the staircase function ($2e_1$), (d) using the staircase function ($2e_1$) with the 1V driving pulse for, (e) using the staircase function ($2e_2$), (f) using the staircase function ($2e_2$) with 1V driving pulse for. Note that all subfigures: $x = 1\text{ V/div}$ and $y = 1\text{ V/div}$.

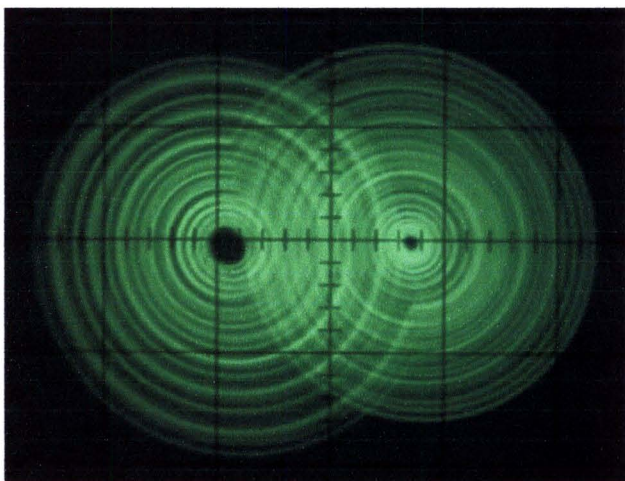


Fig. 17. Experimental results of the system Model III. Note that axes $x = 2\text{ V/div}$ and $y = 1 = 2\text{ V/div}$.

variety of choices as the Heaviside, the signum, the hysteresis and the saturate functions having voltage gains 5 and 7. The results of this experiment are shown in Figs. 14(a)–14(e) respectively. The four-scroll chaotic attractor is also shown in Figs. 14(f) and 14(g) achieved by using the signum function in system Model I with 2 V driving external pulse signals for $x_p(t)$ and $y_p(t)$.

By replacing the programmable nonlinear function in Model I with the staircase function, the chaotic system can be obtained as a 3-scroll and 4-scroll attractor as shown in Figs. 15(a) and 15(b) by applying voltage level at the terminal V_c of

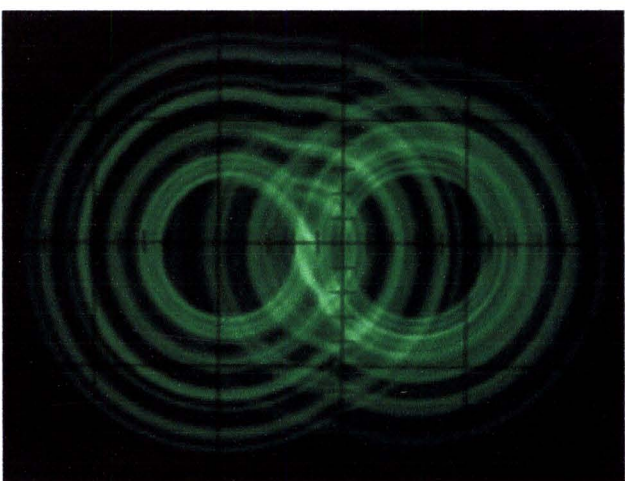
the staircase function module. Figures 15(c), 15(d), 15(f) and 15(g) are the 6-scrolls and the 8-scrolls generated from the system in Model I having the nonlinear equations (2e₁) and (2e₂) by driving external pulse signals to the terminals $x_p(t)$ or $y_p(t)$. Figures 15(e)–15(h) are two-dimensional grid scrolls which can be obtained by applying pulse signals to both $x_p(t)$ and $x_p(t)$.

5.2. Results from Model II

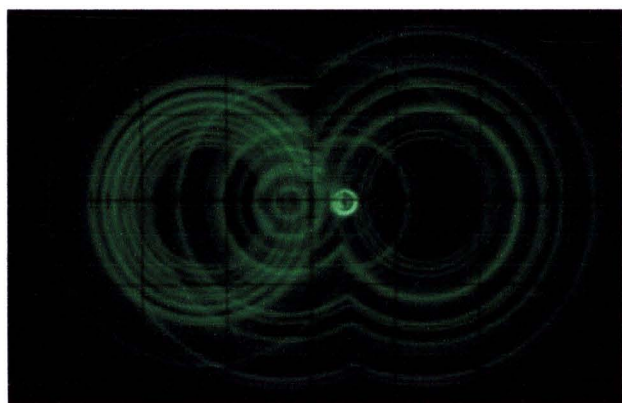
Figure 16(a) shows the result of the experimental set up corresponding to Fig. 9 for Model II, which is a double-scroll chaotic attractor obtained by using the signum function. In addition, experimental results of the system Model II using the staircase function is a 3- or 4-scroll chaotic attractor shown in Figs. 16(c) and 16(e). To increase the number of scrolls of both systems in Model II using the signum and the staircase functions, multiscroll attractors are shown in Figs. 16(b), 16(d), 16(f), that are obtained as the extended forms of double-, 3- and 4-scroll systems in Figs. 16(a), 16(c), 16(e) along the y -axis by injecting the external pulse signal to the terminal $y_p(t)$ in the main module.

5.3. Results from Model III

Figure 17 shows the results of the chaotic oscillator in system Model III. Figures 18(a) and 18(b) show

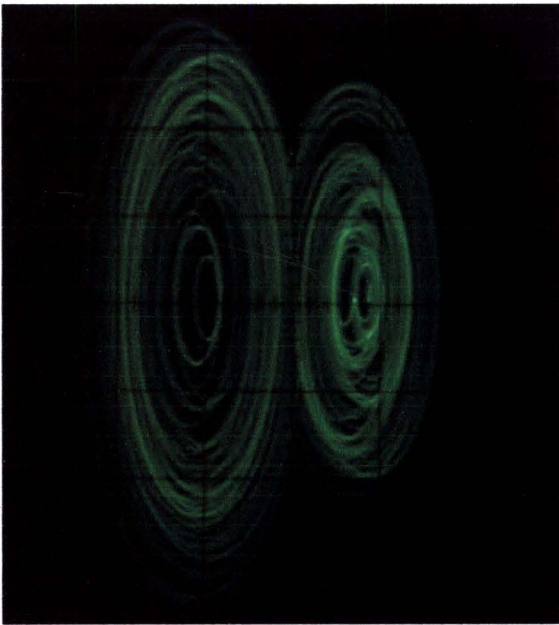


(a)

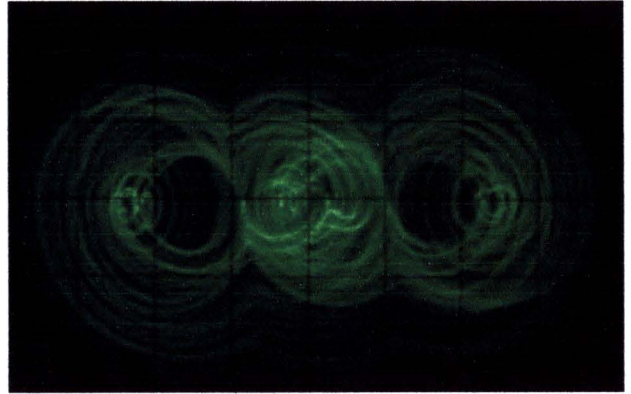


(b)

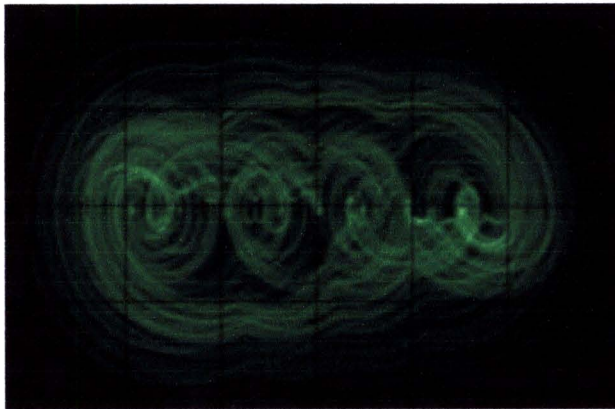
Fig. 18. Experimental results of the system Model IV: (a) using the Heaviside function with the driving pulse signal, (b) using the signum function with the driving pulse signal, (c) using the signum function with the driving sinusoidal signal, (d) using the staircase function (2e₁) with the driving sinusoidal signal, (e) using the staircase function (2e₂) with the driving sinusoidal signal. Note that $x = 2\text{ V/div}$ and $y = 2\text{ V/div}$.



(c)



(d)



(e)

Fig. 18. (*Continued*)

results of the experimental setup corresponding to the nonautonomous chaotic oscillator excited by the external pulse signal with the Heaviside or the signum functions, respectively.

5.4. *Results from Model IV*

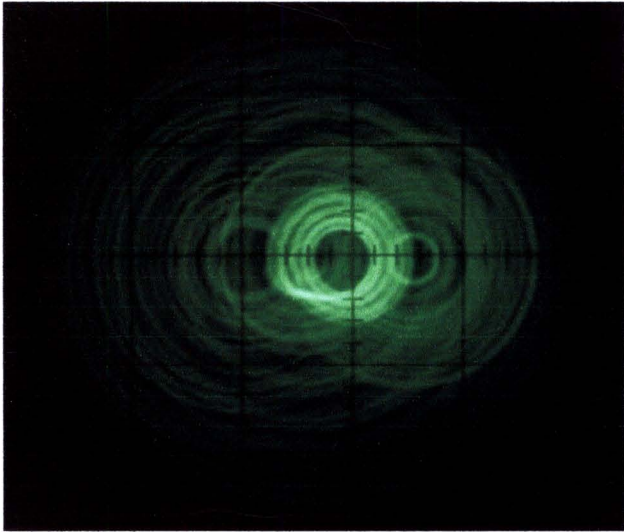
In Fig. 18(c), a double-scroll chaotic oscillator is obtained from the nonautonomous chaotic system using the signum function with the sinusoidal signal driving force. By using the staircase module instead, 3- and 4-scrolls are obtained and shown in Figs. 18(d) and 18(f).

5.5. *Results of the mixed-mode models*

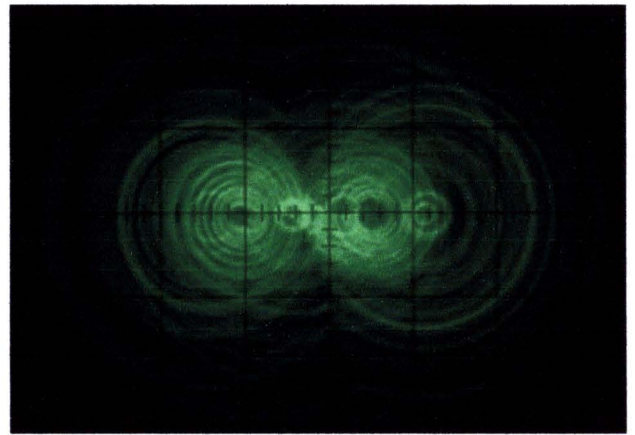
For a mixed-mode chaotic oscillator, results of the experimental set up of Scheme 1 which is the third-order autonomous chaotic system mixed with a second-order nonautonomous chaotic system with the pulse excitation using the Heaviside and the signum functions as the nonlinear elements are shown in Figs. 19(a) and 19(b), respectively. For the mixed-mode Scheme 2 the nonautonomous chaotic system Model IV is excited with the signum function by the sinusoidal signal, the results of the experimental is shown in Fig. 19(c).

Figures 19(d) and 19(e) are the 3 and 4-scroll chaotic attractors obtained from the experimental set up of the mixed mode Scheme 3, where the staircase function and the external pulse driving force are used to compose the main module. Finally

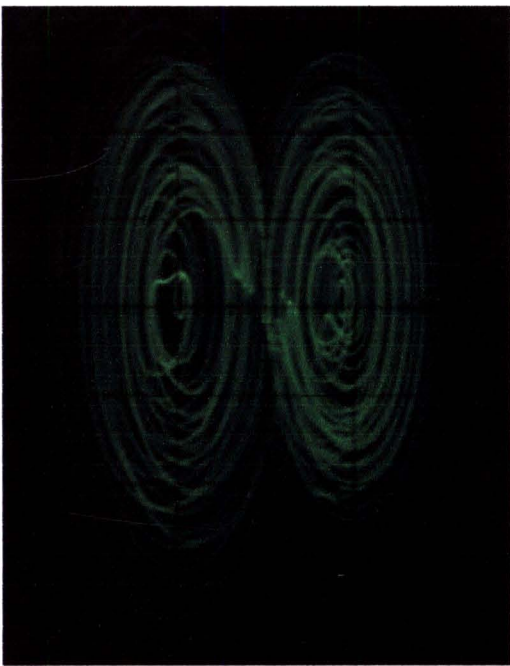
the pseudo 7-scroll chaotic pattern obtained from toggling an analog multiplex switch in the nonlinear module multiscroll chaotic system in Models I and II is shown in Figs. 19(f) and 19(g). As can be seen in the figures that the real 3-scroll and 4-scroll



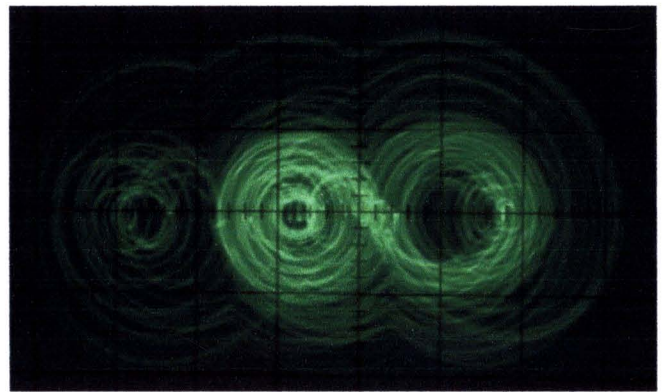
(a)



(b)

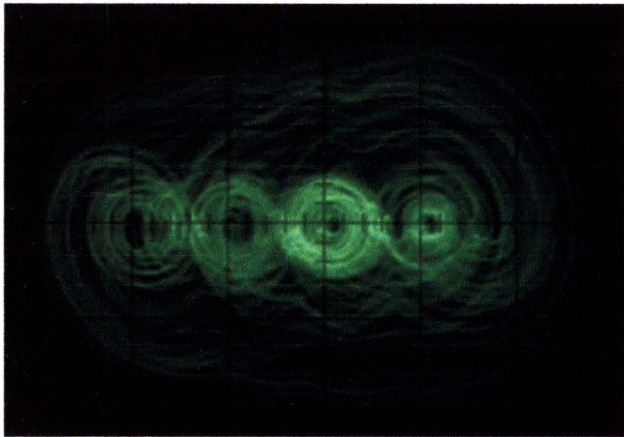


(c)

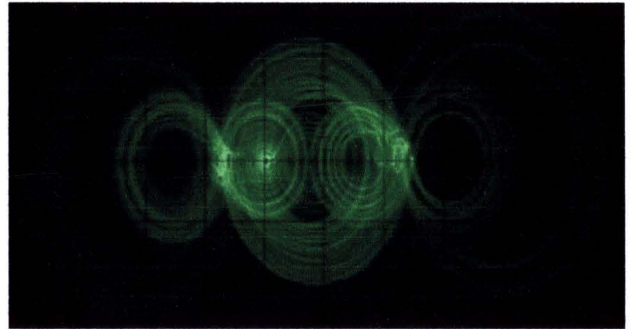


(d)

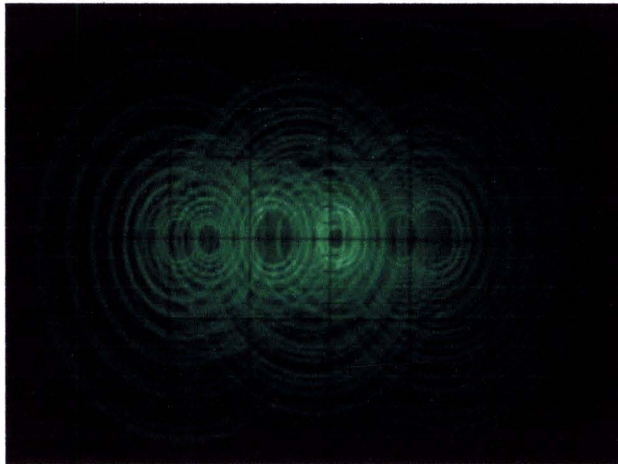
Fig. 19. Experimental results of the mixed-mode chaotic circuit: (a) Scheme 1 using the Heaviside function (b) Scheme 1 using the signum function (c) Scheme 2 (d) Scheme 3 using the staircase function ($2e_1$) (e) Scheme 3 using the staircase function ($2e_2$) (f) The pseudo 7-scroll pattern using the staircase functions ($2e_1$) and ($2e_2$) (g) The pseudo 7-scroll pattern using the staircase functions (4a) and (4b).



(e)



(f)



(g)

Fig. 19. (Continued)

patterns are visualized by adding to 7-scrolls. The fast switching effect cannot be caught in a snapshot even by an analog 200 Hz oscilloscope.

6. Conclusions

The objective of this work is to design and construct a few block modules that can generate many chaotic signals for engineering students at the undergraduate level. The pedagogy and teaching strategy for using these proposed tool kits are carried out by considering students' background in the second-order dynamic system or a feedback system. Under this assumption, the chaotification approach can be alternatively introduced rather than using the well-known Chua's circuit for conducting the laboratory experiment. For fruitful learning results, students are first introduced to system models and

then the property is explored and philosophy of the circuit modules designed and its topological terminology.

Familiarizing with the circuit modules, the students are then encouraged to experiment by composing the modules corresponding to the various system models for constructing various chaotic patterns as simple as wire jumping to interconnecting the subsystems. In this paper, more than 30 chaotic patterns can be obtained from possible combination of only the four block modules. Each module is cost-effective, so relatively inexpensive multipliers are required and is easy-to-implement by using only a few op-amps. Simulation results agree with the experiment revealing the effectiveness of the designed educational kit. The readers are encouraged to construct the kit by using the design guideline provided in this paper.

Acknowledgments

This research is supported by Thailand Research Fund under grant RGJ-PhD/231/2547 and the NRCT grant for the fiscal years of 2553 and 2554.

References

- Addabbo, T., Fort, A., Rocchi, S. & Vignoli, V. [2010] "Exploiting chaotic dynamics for A-D converter testing," *Int. J. Bifurcation and Chaos* **20**, 1099–1118.
- Bilotta, E., Bossio, E. & Pantano, P. [2010] "Chaos at school: Chua's circuit for students in junior and senior high school," *Int. J. Bifurcation and Chaos* **20**, 1–28.
- Buscarino, A., Fortuna, L., Frasca, M. & Muscato, G. [2007] "Chaos does help motion control," *Int. J. Bifurcation and Chaos* **17**, 3577–3582.
- Chaturvedi, D. K. [2010] *Modeling and Simulation of Systems Using MATLAB and Simulink* (CRC Press, FL).
- Cook [1985] "Simple feedback systems with chaotic behavior," *Syst. Contr. Lett.* **6**, 223–227.
- Dewey, J. [1938] *Experience and Education* (McMillan, NY).
- Ditto, W. L., Murali, K. & Sinha, S. [2008] "Chaos computing: Ideas and implementations," *Phil. Trans. R. Soc. A* **366**, 653–664.
- Elwakil, A. S. & Kennedy, M. P. [2001] "Construction of classes of circuit independent chaotic oscillators using passive-only non-linear devices," *IEEE Trans. Circuits Syst.-I* **48**, 289–307.
- Gray, P. O. [2010] *Psychology*, 6th edition (Worth Publishers, NY).
- Hirsch, M. W. & Smale, S. [1974] *Differential Equations, Dynamical Systems and Linear Algebra* (Academic Press, NY).
- Hong, L., Zhong, L., Zhang, B., Wang, F., Tan, N. & Halang, W. A. [2010] "Design of analogue chaotic PWM for EMI suppression," *IEEE Trans. EMC* **52**, 1001–1007.
- Kiliç, R. [2010] *A Practical Guide for Study Chua's Circuits* (World Scientific, Singapore).
- Lewis, F. L. & Syrmos, V. [1995] *Optimal Control*, 2nd edition (John Wiley and Sons, NY).
- Liu, Z., Zhu, X. H., Hu, W. & Fei, J. [2007] "Principles of chaotic signal radar," *Int. J. Bifurcation and Chaos* **17**, 1735–1739.
- Lü, J. H., Murali, K., Sinha, S., Leung, H. & Aziz-Alaoui, M. A. [2008] "Generating multiscroll chaotic attractors by thresholding," *Phys. Lett. A* **372**, 3234–3239.
- Ma, H. G., Zhua, X. F., Xua, J. F. & Ai, M. S. [2008] "Circuit state analysis using chaotic signal excitation," *J. Franklin Inst.* **345**, 75–86.
- Milioua, A. N., Antoniadessa, I. P., Stavrinides, S. G. & Anagnostopoulos, A. N. [2007] "Secure communication by chaotic synchronization: Robustness under noisy conditions," *Nonlin. Anal: Real World Appl.* **8**, 1003–1012.
- Mohamed, I. R., Murali, K., Sinha, S. & Lindberg, E. [2010] "Design of threshold controller based chaotic circuits," *Int. J. Bifurcation and Chaos* **20**, 2185–2191.
- Moreno, U. F., Peres, P. L. D. & Bonatti, I. S. [2001] "Analysis of piecewise-linear oscillators," *IEEE Trans. Circuits Syst.-I* **50**, 1120–1124.
- Mykolaitis, A., Tamasevicius, A., Namajunas, A., Cenys, A. & Anagnostopoulos, A. [2000] "Non-autonomous 2nd order chaotic circuit with comparator," *IEE Proc. G Circuits, Devices Syst.* **147**, 291–292.
- Ozoguz, S. & Elwakil, A. S. [2004] "On the realization of circuit-independent nonautonomous pulse-excited chaotic oscillator circuits," *IEEE Trans. Circuits Syst.-II* **51**, 552–556.
- Sooraksa, P. & Klomkarn, K. [2010] "No-CPU chaotic robots: From classroom to commerce," *IEEE Circuits Syst. Mag.* **10**, 46–53.
- Sprott, J. C. [2000] "Simple chaotic systems and circuits," *Amer. J. Phys.* **68**, 758–763.
- Tam, W. M., Lau, F. C. M. & Tse, C. K. [2006] *Digital Communications with Chaos: Multiple Access Techniques and Performance* (Elsevier, Amsterdam).
- Tamaševičius, A., Mykolaitis, G., Pyragas, V. & Pyragas, K. [2005] "A simple chaotic oscillator for educational purposes," *Eur. J. Phys.* **26**, 61–63.
- Tang, K. S. & Zhong, G. Q. [2003] "Chaotification of linear continuous-time systems using simple nonlinear feedback," *Int. J. Bifurcation and Chaos* **13**, 3099–3106.
- Tôrres, L. A. B. & Aguirre, L. A. [2005] "PC ChuaA laboratory setup for real-time control and synchronization of chaotic oscillators," *Int. J. Bifurcation and Chaos* **15**, 2349–2360.
- Yalcin, M. E., Suykens, J. A. K., Vandewalle, J. & Ozoguz, S. [2002] "Families of scroll grid attractors," *Int. J. Bifurcation and Chaos* **12**, 23–41.
- Yalcin, M. E., Suykens, J. A. K. & Vandewalle, J. [2004] "True random bit generation from a double-scroll attractor," *IEEE Trans. Circuits. Syst.-I* **51**, 1395–1404.
- Yu, S. M., Lü, J. H., Leung, H. & Chen, G. [2005] "Design and implementation of n -scroll chaotic attractors from a general jerk circuit," *IEEE Trans. Circuits Syst.-I* **52**, 1459–1476.
- Yu, S. M., Lü, J. H. & Chen, G. [2007] "A module-based and unified approach to chaotic circuit design and its applications," *Int. J. Bifurcation and Chaos* **17**, 1785–1800.
- Zhang, Z. & Chen, G. [2007] "Chaotic liquid shaker: Design, implement and application," *Int. J. Bifurcation and Chaos* **17**, 4443–4451.

เอกสารแนบหมายเลข 3

ผลงานที่ได้จากทุนวิจัยได้รับรางวัลนวัตกรรมต้นแบบยอดเยี่ยมด้าน

โทรคมนาคมจาก TRIDI

ประมวลภาพงานผลการตัดสินรางวัล Telecommunication Innovation
Award ณ. ห้างเอสพานาด ถ.รัชดา วันที่ 26 พ.ย. 2553



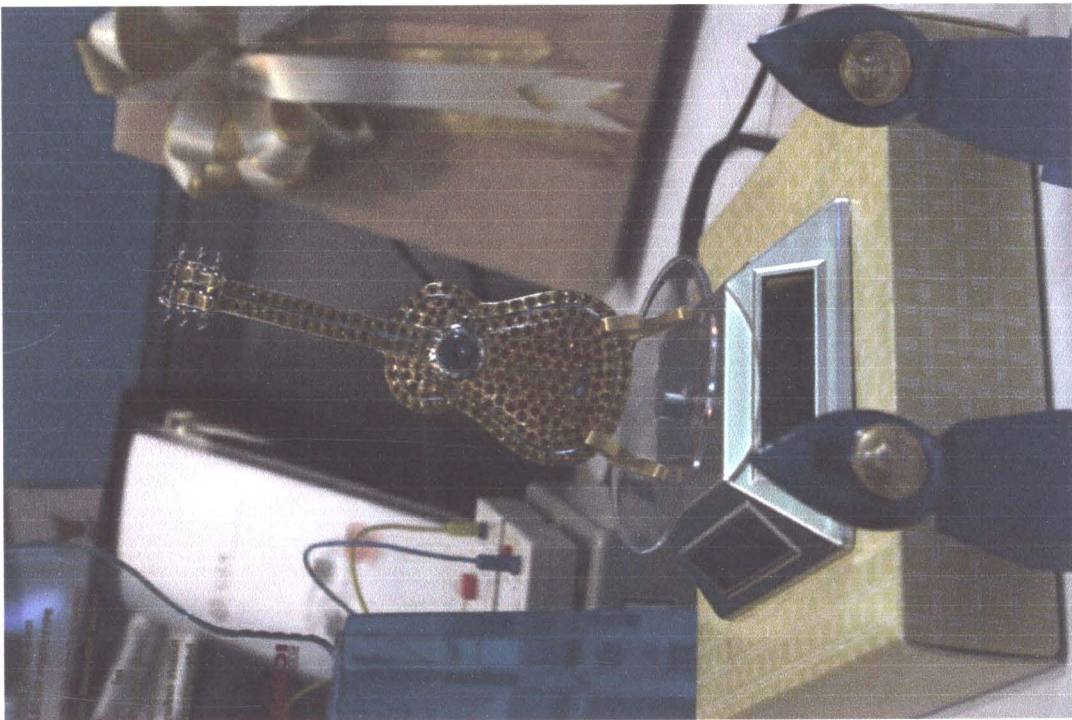
บูธจัดแสดงในนาม สถาบันเทคโนโลยีพระจอมเกล้า - ลาดกระบัง



รศ.ดร. ปิติเขต สุรรักษา หัวหน้าทีมรับรางวัลยอดเยี่ยมประเภท telecom
proto-type จาก พอ.ดร. นที ศุกลรัตน์ กรรมการ กทช



VDO รศ.ดร. ปิติเชต สุ์รักษา ให้สัมภาษณ์ สื่อมวลชน



ตัวต้นแบบอุปกรณ์เข้ารหัสลับด้วยสัญญาณอลวน (chaotic encryption device) ที่ได้รับทุนจากสภาวิจัย ประจำปี 2553

